Report 1862

PRELIMINARY EXPERIMENTS FOR CRATER MODELING IN CONTROLLED SOIL MEDIA

by

George Gornak

June 1966

U. S. ARMY ENGINEER RESEARCH AND DEVELOPMENT LABORATORIES
FORT BELVOIR, VIRGINIA

U. S. ARMY ENGINEER RESEARCH AND DEVELOPMENT LABORATORIES
FORT BELVOIR, VIRGINIA

Report 1862

PRELIMINARY EXPERIMENTS FOR CRATER MODELING IN CONTROLLED SOIL MEDIA

Task 1N022601A08906

June 1966

Distributed by

The Commanding Officer
U. S. Army Engineer Research and Development Laboratories

Prepared by

George Gornak
Combat Research Division
Military Department

SUMMARY

This report covers a series of 30-gram, high-explosive cratering tests performed to determine the effect soil moisture content in relation to the soil's plastic limit has on craters, ground shock velocities, residual displacements, and the rarefaction wave.

The report concludes:

a. In a cohesive soil the moist condition (moisture content within the plastic index) as contrasted with the dry condition (moisture content well below the plastic limit) influences crater formation in the following ways.

(1) Fallback into the crater is reduced so that apparent and true crater dimensions are identical.

(2) The profile of the crater is more symmetrical and parabolic in shape.

(3) The ejecta which consist of large clods, for the most part, are distributed near the crater lip.

(4) The crater parameters of depth, diameter, and especially volume are considerably increased.

(5) Attenuation rate of the shock velocity is lessened appreciably and results in higher shock velocities and pressures at greater distances from the center of the charge.

(6) Larger soil displacements are obtained at any given distance from the center of the charge.

(7) The possibility exists that a substantial increase in residual radiation may result from the lack of fallback material.

b. Large-scale results in marine muck and silty sand compared with results of this study reveal similarity in crater form. This suggests a general hypothesis that any soil which has moisture content that approaches the plastic limit will exhibit similar behavior.

FOREWORD

The investigation reported herein was authorized and accomplished as a part of U. S. Army Materiel Command Task 1N022601A08906, "Atomic Demolition Munition Effects Research." A copy of the task card is included as Appendix A.

Tests were conducted at the Barrier Experimental Facility, U. S. Army Engineer Research and Development Laboratories' North Annex during 22 April through 11 November 1964.

The investigation was conducted with the able assistance of the 73rd Engineer Company in grading the soil media; Pfc Jesse Reese and Pfc Robert Weaver of the 87th Construction Battalion in preparing the soil media; and Thomas J. Johnson, David Clegg, and Bert Sheets of the Barrier Experimental Facility in careful implementation of all their assigned duties throughout a tedious program. James B. Duff, Computation and Analysis Division, performed the statistical analysis of the crater data.

CONTENTS

Section	Title	Page
	SUMMARY	ii
	FOREWORD	iii
I	INTRODUCTION	
	1. Subject	1
	2. Background and Previous Investigations	1
II	INVESTIGATION	
	A. TEST PROCEDURES	
	3. Preliminary HE Tests	2
	4. Preliminary Time-of-Arrival Gage Tests	4
	5. Site Preparation	5
	6. Material Preparation	7
	7. Time-of-Arrival Gage Installation	9
	8. Cratering and Crater Measurements	12
	B. TABULATED TEST DATA	
	9. Crater Nomenclature	17
	10. Crater Depth and Diameter Dimensions	17
	11. Remaining Crater Dimensions	17
	12. Crater Volumes	17
	13. Soil Property Data	17
	14. Soil Characteristics Data	17
	15. Time-of-Arrival Data	17
	16. Gage Displacement Data	17
III	DISCUSSION	
	17. Adequacy of Methods and Equipment	17
	18. Crater Profiles	30
	19. Crater Diameters	32
	20. Crater Depths	36
	21. Crater Volumes	38

CONTENTS (cont'd)

Section	Title	Page
	22. Time-of-Arrival Data and Shock Velocities	40
	23. Net Gage Displacements	42
	24. Rarefaction Wave	45
	25. Soil Properties	47
IV	CONCLUSIONS	
	26. Conclusions	48
	LITERATURE CITED	49
	APPENDICES	
	A. Authority	50
	B. Profiles of Resulting Craters	
	1 through 8, Dry Media	51-58
	9 through 17, Wet Media	59-67
	C. Supplementary Information: Statistical Analysis of Cratering and Soil Data	68

ILLUSTRATIONS

Figure	Title	Page
1	Explosive Charge; 30 g of Composition C-4 Explosive, Molded in Sphere, Primed with No. 6 Commercial DuPont Electric Blasting Cap	3
2	Detonation Products of 30-g Charge Photographed at 3.0×10^{-6} Sec	4
3	Various Stages in Preparing Strain Gages	5
4	Arrangement of Test Site	6
5	Improvised Wide-Flange Platform Scale	9
6	Steel and Plexiglas Frame Used in Making Gage Core	10
7	Replacing Soil with Equal Volume of 90 SAE Weight Oil	11
8	Wet Gage Core Before Its Installation in Soil	13
9	Depth Gage and Steel Angle Used in Measuring Craters	14
10	Time-of-Arrival Oscilloscope Traces Obtained with Strain Gages	15
11	Crater Nomenclature	16
12	Crater Produced at Depth of Burst of 9.3 cm	31
13	Results of Large-Scale Cratering Tests Conducted at Panama Canal	33
14	Crater Phenomena at Panama Canal	34
15	Depth of Burst vs Crater Diameter	35
16	Depth of Burst vs Crater Depth	37

ILLUSTRATIONS (cont'd)

Figure	Title	Page
17	Depth of Burst vs Crater Volume	39
18	Distance between Center of Charge and Gage vs Time of Arrival	40
19	Radius vs Shock Velocity	42
20	Distance between Bottom of Charge and Gage vs Net Gage Displacement in Wet and Dry Media	43
21	Distance between Bottom of Charge and Gage vs Net Gage Displacement with Various Depths of Burst in Wet Soil	44
22	Idealized Scaled Depth of Burst vs Crushing Radius	46
23	Scaled Depth of Burst vs Scaled Crushing Radius	47

TABLES

Table	Title	Page
I	Crater Measurements for Soil Moisture Content of 10.6 Percent	18
II	Crater Measurements for Soil Moisture Content of 21.0 Percent	19
III	Other Crater Measurements for Soil Moisture Content of 10.6 Percent	20
IV	Other Crater Measurements for Soil Moisture Content of 21.0 Percent	21
V	Apparent and True Crater Volumes for Soil Moisture Content of 10.6 Percent	22
VI	Apparent and True Crater Volumes for Soil Moisture Content of 21.0 Percent	22
VII	Sieve Analysis of Samples of Soil Media	23
VIII	Soil Characteristics for Soil Moisture Content of 10.6 Percent	24
IX	Soil Characteristics for Soil Moisture Content of 21.0 Percent	25
X	Time of Arrival for Soil Moisture Content of 10.6 Percent	26
XI	Time of Arrival for Soil Moisture Content of 21.0 Percent	27
XII	Net Gage Movement for Soil Moisture Content of 10.6 Percent	28
XIII	Net Gage Movement for Soil Moisture Content of 21.0 Percent	29
XIV	Dependent and Independent Variables with Supplementary Information on Soil Samples	68-69
XV	Soil Sample Size, Mean, and Standard Deviation	71
XVI	Analysis of Variance	71
XVII	Resultant Means and Standard Deviations of Soil Samples	72

PRELIMINARY EXPERIMENTS FOR CRATER MODELING IN CONTROLLED SOIL MEDIA

I. INTRODUCTION

1. Subject. This report covers a series of 30-gram, high-explosive (HE) cratering tests performed to determine the effect soil moisture content in relation to the soils' plastic limit has on craters. ground shock velocities, residual displacements, and the rarefaction wave.

2. Background and Previous Investigations. Under an Army RDT&E task, "Atomic Demolition Munition Effects Research," small high-explosive tests were conducted for Project ADMIRALS (ADM Induced Rock and Land Slides) during the spring and fall of 1962. While these tests were being conducted, variations in the test data were detected, but these anomalies were not extensively analyzed at that time.

At the 32nd Symposium on Shock, Vibration, and Associated Environments on 15 April 1963, Porzel (1) presented his paper, "Surface Rarefaction Model for Cratering," which offered a possible explanation of the anomalies.

Using the rarefaction model for cratering as suggested by Porzel and the data obtained earlier, P. J. Morris (2) stated in his Branch report, "Memoranda on Anomalies in Crater Data," that formation of a rarefaction wave is sensitive to soil moisture content in relation to the soils' plastic limit. Morris suggested that cratering in soils with moisture contents at or approaching the plastic limit of the soils would result in more material being ejected from the crater by the rarefaction wave and would thus give rise to a larger apparent crater but a shallower true crater.

To evaluate this hypothesis, an exhaustive literature search was made to obtain all crater data that were available. Once the data were obtained they were found to be of little use because conditions from test to test varied, and all the information needed to evaluate the hypothesis was not required or obtained during most of these tests.

As a result of this lack of information, the Project Engineer decided that a limited amount of small HE tests could be designed and conducted to provide crater information in controlled soil media which could be used to evaluate the hypothesis.

The approach was to provide a constant explosive energy source and obtain soil media, the material properties of which remain homogeneous while only the explosive's depth of burst (Dob) and soil moisture content vary. Measurements were to be made of the soil properties desired, shock velocities, crater dimensions, and residual displacements.

Prior to these tests, reproducibility of the crater dimensions was established as the criterion for determining the success of the investigation. Examination of the variables established charge detonation reliability, shock wave configuration, soil moisture content, soil consistency, and soil density as the most important items affecting reproducibility. When reproducibility had been established as the criterion, techniques were devised for controlling and monitoring the variables affecting reproducibility.

II. INVESTIGATION

A. TEST PROCEDURES

3. Preliminary HE Tests. Tests were conducted during a period 22 April through 11 November 1964 to determine the smallest spherical explosive source that could be detonated reliably and also provided a means for determining the volume of soil required for the investigation.

The explosive, C4* was selected as the explosive energy source. Its selection was governed by its availability and by USAERDL test personnel's previous experience which indicated that C-4 could be initiated by means of a commercial No. 6 DuPont electric blasting cap.

The desired production of a near spherical shock wave and reliable detonation dictated the location of the initation point. The minimum 2.0-centimeter radius was used for attaining maximum detonation velocity as given by Cook (3) and the blasting cap was centrally positioned so that a minimum of 2.0 centimeters remained between the bottom of the blasting cap and the explosive charge (Fig. 1).

Figure 2 shows the near spherical detonation products obtained approximately 3.0 microseconds after detonation. The shock front cannot

* The composition of C4 is as follows: RDX, 91.00 percent; Polyisobutylene, 2.10 percent; motor oil, 1.60 percent; and di-(2-ethylhexyl) sebacate, 5.30 percent.

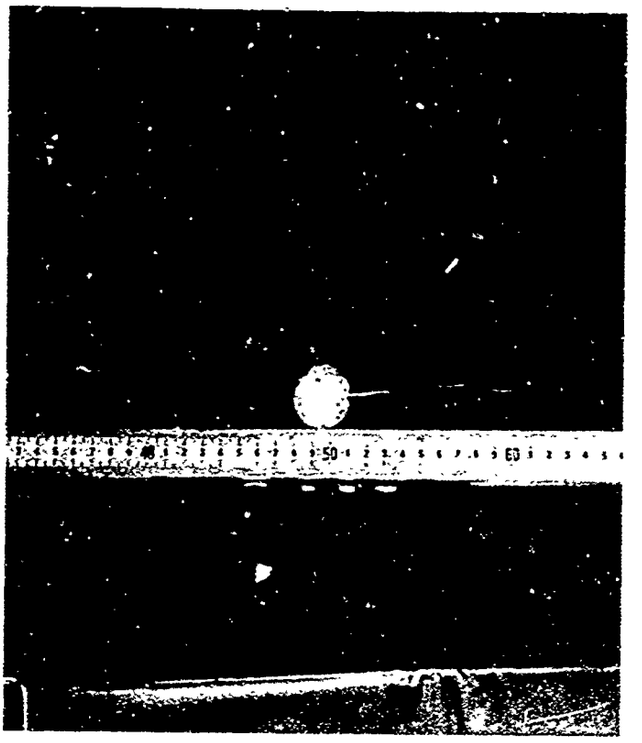

L9520

Fig. 1. Explosive charge; 30 g of Composition C-4 explosive, molded in sphere, primed with No. 6 commercial DuPont electric blasting cap.

be seen in the photograph, but it can be expected to be as near spherical as the detonation products, especially when confined as in the soil media.

After the explosive initiator and initiation point had been determined, twenty-four 20-gram charges were detonated in an undisturbed, thoroughly rain-soaked, sandy clay located on Range 1 of the North Annex of these Laboratories. The tests indicated that charges could be reliably detonated with the No. 6 electric blasting cap. A 30-gram explosive charge was finally selected because of the ease of handling a larger size charge.

Dimensions of the proposed soil container were determined by measuring the maximum crater parameters produced and comprehending problems associated with the reflected shock waves. The width and length of the container were set at 7 feet, while the depth was reduced to 4 feet. The reduction in the depth was believed permissible because the bottom of the container would be open; thus, the soil medium would remain in direct contact with the existing soil.

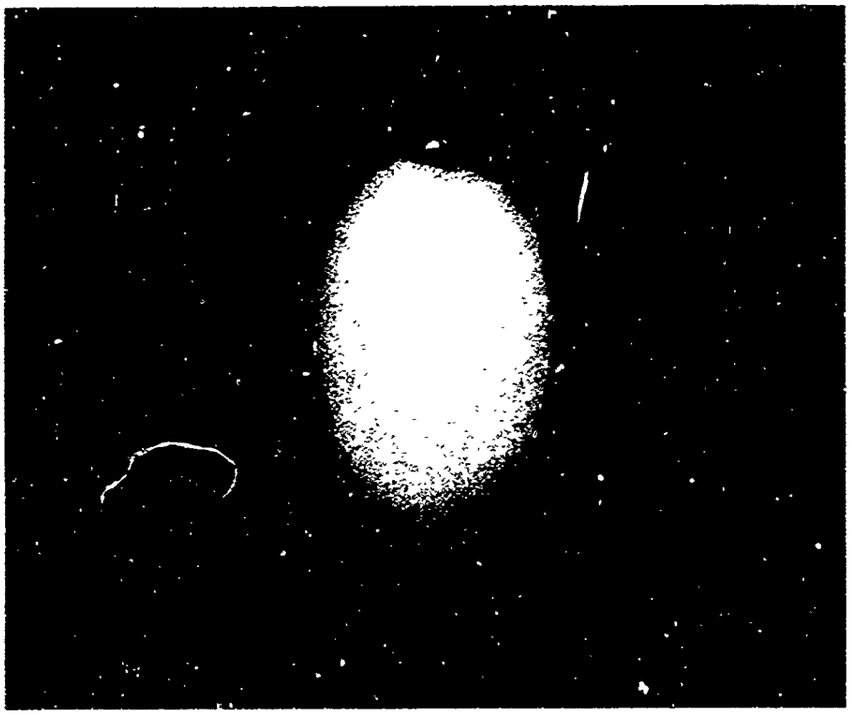

Fig. 2. Detonation products of 30-g charge photographed at 3.0×10^{-6} sec.

4. Preliminary Time-of-Arrival Gage Tests. To observe the behavior of the ground shock velocity with soil moisture content, test personnel had to select a suitable time-of-arrival gage which would meet the criteria of rapid response, water tightness, and small size; would match soil impedance; and above all, would be inexpensive. Once selected, the gage and the associated circuit would be tested with the explosive source previously chosen.

Accelerometers were considered to be too expensive; therefore, SR-4 wire strain gages, Baldwin-Lima-Hamilton, type A-5, were selected to be used during the preliminary tests (Fig. 3). Each gage was prepared by removing the felt protector, trimming the paper backing to an approximate size of 1/4 inch wide by 3/8 inch long, immersing each one in a silicon rubber compound, and finally curing the rubber compound for a 24-hour period. The approximate thickness of the gages after potting was 1/8 inch. The gages were then attached to 12 feet of RG-174/U coaxial cable and made the variable part of the dynamic strain gage circuit.

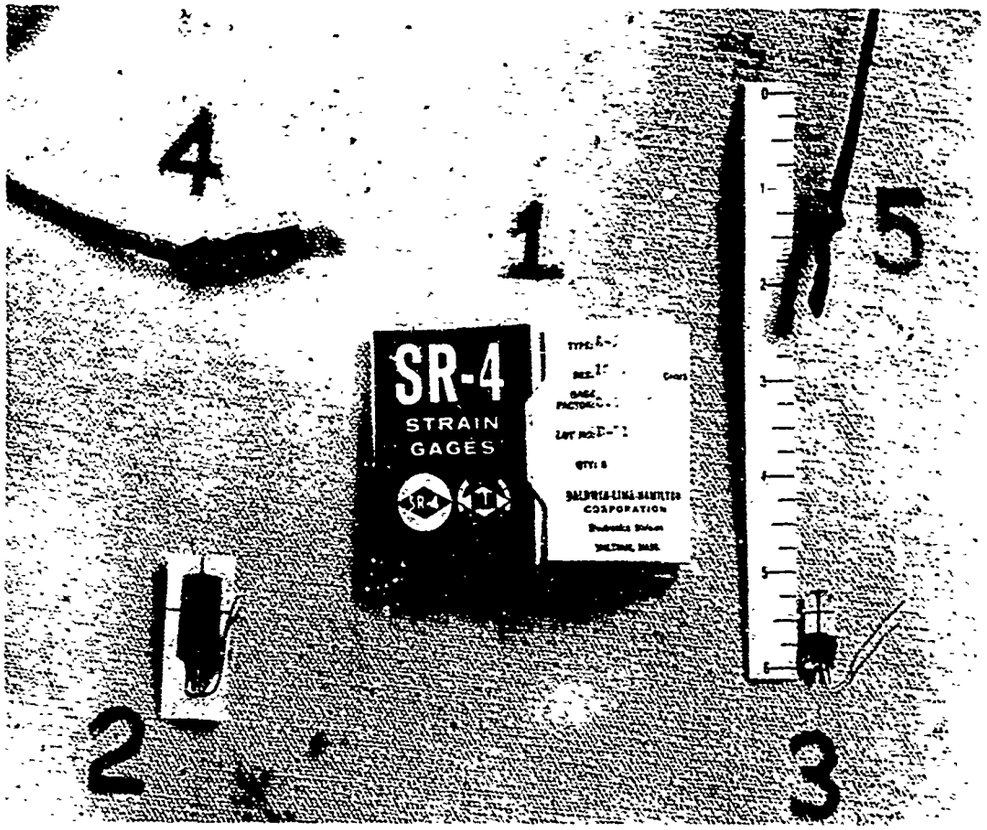

L9562

Fig. 3. Various stages in preparing strain gages.

These gages were then carefully placed at extreme and moderate distances from the explosive source while a T-1 target was placed at the bottom of the charge to indicate emergence of the shock wave from the explosive to the soil medium. This procedure was employed to detonate approximately twelve 30-gram C4 spherical charges, and these tests indicated that the SR-4 gage would be sensitive enough to indicate shock wave velocities at a depth of 40.0 centimeters beneath the bottom of the explosive source.

5. Site Preparation. An area on Range 2 of the USAERDL North Annex was excavated to an approximate depth of 2 feet and graded level to facilitate the positioning of two plywood, open end soil containers. They were braced at the third points with wood A frames to prevent damage to the containers during compaction of the soil and the explosive tests. The soil around the containers was brought to grade level, and inside they were

lined with 6-mil-thick plastic film to prevent moisture seeping into or out of them.

Two pitched-roof frame shelters were constructed to prevent excessive drying of the open upper portion of the containers. The frames were covered with canvas and drop cloth plastic. These shelters were also used during preparation of the soil medium before each test.

A 16 S mobile concrete mixer was placed between the two containers and adjacent to a soil stockpile. A sheet metal extension spout was built to convey the mixed soil from the discharge end of the mixer to either soil container. A skip was mounted on the other end of the mixer for receiving the soil and transferring it into the mixing drum. At this end, a hopper was placed on four calibrated load cells to permit the soil to be weighed prior to mixing. The stockpile of bulk soil and a crane were positioned adjacent to these items. A 10,000-gallon water tank trailer was positioned to the opposite side of the mixer and hopper. The test site is shown in Fig. 4.

L9511

Fig. 4. Arrangement of test site.

Coinciding with these operations, calibration of the existing water gage on the 16 S mobile concrete mixer was begun. The gage is used to predetermine the amount of water in gallons or pounds to be discharged into the mixing drum of the mixer. The gage was set at various positions, and repeated discharges were made and weighed. The gage readings were found to be erratic with as much as 12 percent variation from one discharge to the next.

Therefore, a visual water gage which originally consisted of a plain glass tube adjacent to the overhead water tank was replaced. Instead of the glass tube, a Plexiglas tube of the appropriate diameter was scribed in 1/4-inch increments for a length of 11 inches and inserted in its place. The weights of the discharge water were checked between various increments of the Plexiglas gage and were found to be consistent from one discharge to the next. Results were then tabulated and used during the entire test program.

6. Material Preparation. The need was realized for a consistent soil medium which would exhibit the properties of a cohesive soil which has a plastic limit and a liquid limit; hence, test personnel decided to use the soil available on Range 1 of the North Annex. Previous soil tests indicated the soil possessed a plastic limit and liquid limit at an approximate moisture content of 20 percent and 30 percent, respectively. Thus, an area approximately 120 feet long by 200 feet wide was scraped of a 3-inch layer of weathered top soil which was completely free of vegetation and extremely dry. This exposure ultimately resulted in a soil medium which was comparatively fine and behaved somewhat like talcum powder. This soil was placed in two large, convenient, completely covered piles and awaited screening.

A mobile screening unit was positioned to screen the soil in such manner that only the fines would be conveyed next to the hopper location. Loading of 5-ton dump trucks was alternated from one stockpile to the other, and the soil was transferred to the screening unit where the material was screened and conveyed to the proper covered location near the hopper. The alternate loading was believed to be a desirable feature in obtaining a consistent soil medium. After the screening operation, the soil was also covered with a canvas to preserve its dry state.

While screening and stockpiling operations were continuing, a preliminary soil analysis was made to determine the plastic index and particle gradation, both of which were intended to be consistent throughout the operations. An analysis indicated a plastic index of 4 with a plastic limit of approximately 18 percent and a liquid limit of approximately 22 percent.

Using the preliminary soil analysis data, test personnel decided that one of the soil containers would be prepared with a soil moisture content of 10 percent, below the plastic limit; and the other container would be prepared with a soil moisture content of 20 percent, between the plastic limit and the liquid limit of the soil. Realizing the probable handling problems associated with a soil in the plastic range, test personnel decided to prepare the 10-percent mixture first. Sampling of the soil stockpile for moisture content provided the information required for determining the amount of additional water required to bring the soil moisture to the desired 10 percent.

The procedure for the 10-percent material preparation was as follows:

a. The empty hopper was weighed.

b. A full load of soil was emptied into the hopper and weighed.

c. The soil was transferred to the concrete mixer's container, then, into the concrete mixing drum.

d. The amount of water to be added was determined in inches of reduced water column height on the visual water gage.

e. The mixer was started, and the water and soil were placed into the mixing drum at the same time.

f. The addition of water was stopped when the column height dropped to a predetermined level as had been fixed in d.

g. The mixing was continued until the water and soil formed a consistent mixture. This amount was determined by periodic visual inspection.

h. The soil mixture was then emptied from the mixing drum into the soil container, and an approximate 4-inch layer of soil was left to be compacted each time. Samples for soil moisture content were also taken.

i. One compaction pass was made over the material in the north and south directions, and a second pass was made perpendicular to the previous pass by use of pneumatic tamping equipment.

j. The same procedure was used for each additional layer until the box was filled.

The procedure for the 20-percent material preparation was the same except for the method of weighing the material which was accomplished on the improvised wide-flange platform scale shown in Fig. 5. This change was necessitated by the failure of one load cell.

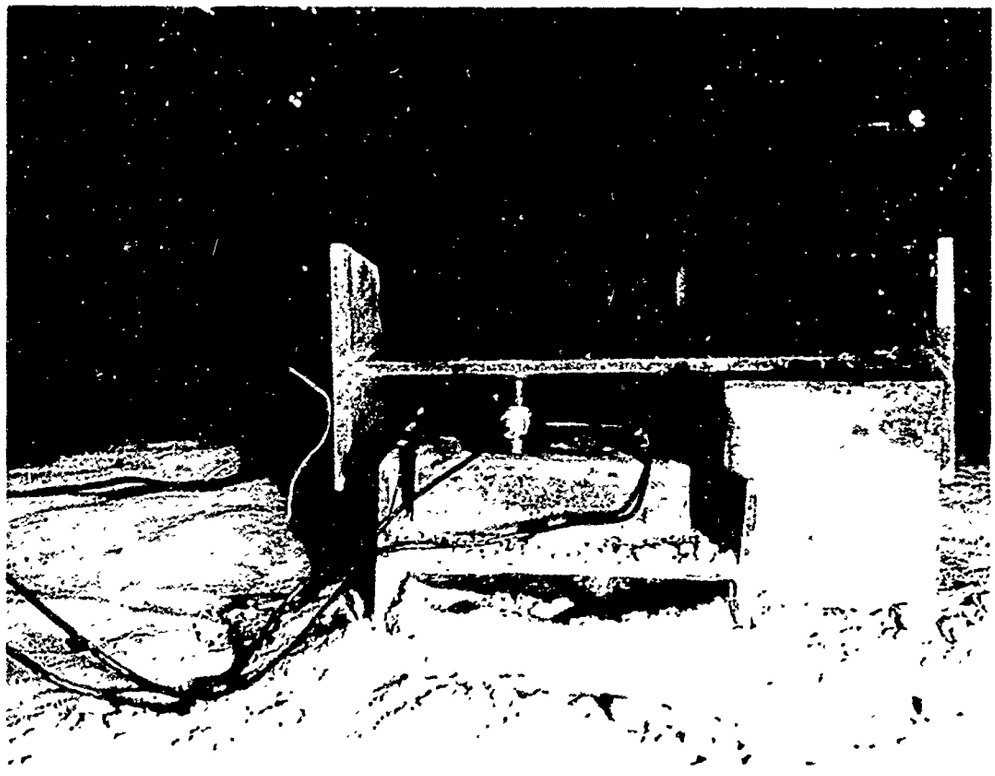

L9501

Fig. 5. Improvised wide-flange platform scale.

Another procedural change was in the method of compaction of the wet medium. The wetted soil formed a spongy mass which resisted compaction efforts when pneumatic equipment was used. Thus, all compaction in the wet medium was accomplished with hand tampers. All other procedures outlined for the dry soil medium were used with success.

7. Time-of-Arrival Gage Installation. Techniques used in this situation are analogous to those methods used in foundry work. Gages were located and tamped in a core made of the mixed soil medium and positioned

in the center of the soil container. At the gage and intermediate positions in the gage core the soil density was checked during the fabrication of the gage core. An exact vertical location of the gages was determined before placing and tamping the surrounding soil media, the density of which was also determined at various positions.

The procedure just summarized is given here in detail. When the soil in the container was brought to a height determined by the deepest time-of-arrival gage the center of the container was found using permanently located points to establish the diagonals and center of the containers. A cord was tautly stretched across each diagonal, and the intersection of these diagonals was located on the soil medium below with a plumb bob. This intersection was used to determine not only the position of the gages but also the T1 target, the 30-gram explosive charge, and the center of the crater.

When the center was established, the area was leveled to receive a steel and Plexiglas core frame (Fig. 6) which had been previously

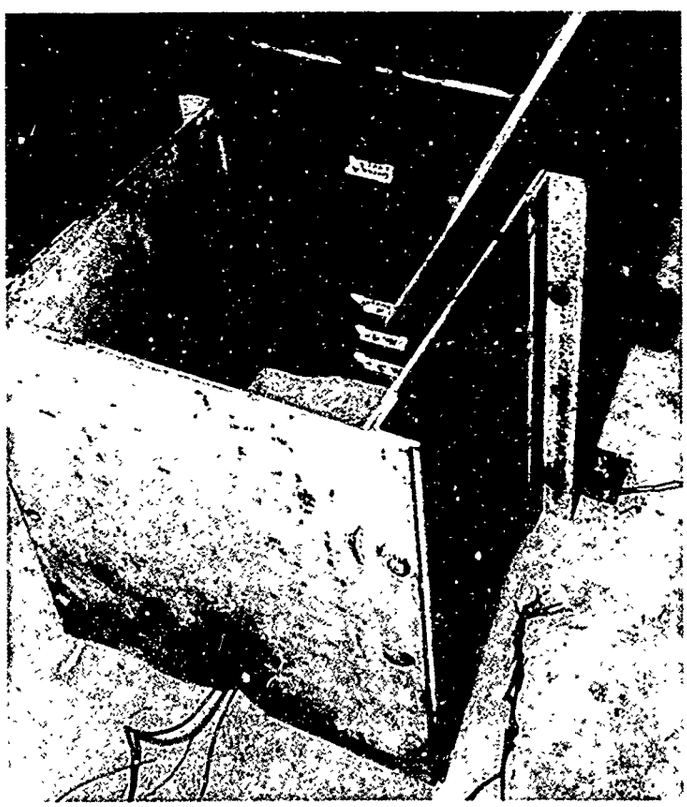

L9573

Fig. 6. Steel and Plexiglas frame used in making gage core.

scribed and marked on the Plexiglas to establish the depth, the center, and the vertical plane of the gages, the T1 target, and the spherical charge. This scribed line was then positioned in the same vertical plane which had been established by the plumbed point on the soil media and the diagonal cord intersection. Once the frame was positioned, approximately 2 to 3 inches of soil media were carefully but firmly tamped around this frame to keep it centered during preparation of the gage core. The mixed soil was then placed in the core frame and tamped until the position of the deepest gage was reached. The gage was positioned, and the coaxial cable was brought out of the prepared opening in the back of the core frame and out of the soil containers. A small amount of soil was placed over the gage and tamped firmly and carefully so as to fix the position of the gage but not to damage it. More soil was added and tamped until the next gage position was reached where the same procedure was used. This process continued until all the gages and T1 targets were emplaced. A wooden, right-semicircular, cylinder core was positioned directly above the T1 target, and then the soil in the core frame was brought to the predetermined ground level in 2-inch increments. The vertical shaft formed by the wooden core was used to position the explosive charge over the T1 target.

During the installation of the gages, soil density was determined at the gages and intermediate positions by removing a small soil core sample and replacing its volume with an equal volume of 90 SAE weight oil (Fig. 7). The weights of wet and dry soils was determined, and standard procedures which permitted determination of the wet and dry densities were used.

L9533

Fig. 7. Replacing soil with equal volume of 90 SAE weight oil.

Once the gage core was completed, the bolted sides of the core frame were removed, and the dimensions from a reference plane were taken to establish the exact location and depth of each of the gages, the T1 targets, and the ground level elevation. The soil media surrounding the core were then carefully placed and tamped in 3-inch layers. Soil density was also taken adjacent to the core and the estimated crater region surrounding this core.

After the charge had been detonated, this procedure was repeated when a considerable amount of disturbed soil media had been removed. The amount of disturbed soil media removed varied with each detonation, but not less than a ton of soil was removed to eliminate variations in the mechanical properties caused by the stress history.

The gage core technique was employed in the wet medium also; however, instead of the Plexiglas and steel frame a 6-inch-diameter cardboard mailing tube was used. The tube was split in half and a slotted section of the back was removed to permit removal of the gage wires. The inside of the tube was marked as to the exact gage, the T1 target, and the ground level location. A layer of graphite was smeared on the inside of the tube to prevent the soil moisture from being absorbed into the cardboard tube. Two halves were then taped together, and a plastic film was placed over the lower end to prevent moisture from escaping from the tube (Fig. 8). The wet soil medium was tamped, and the gages were placed in the same fashion as for dry soil. This gage core was then positioned and the dimensions were determined in the same manner as they had been in the dry soil medium.

Every effort was made to keep the soil medium in the containers at the desired moisture content, but drying occurred and it was necessary to replace approximately 6 inches of the top surface every other cratering test.

8. Cratering and Crater Measurements. A method of measurement consistent with the accuracy desired for these tests and ease of handling was obtained by using a reference plane positioned along the diagonals of the soil containers and a centimeter depth gage. The reference plane used was the horizontal leg of a 3.5- by 3.5- by 0.25-inch structural steel angle. The vertical leg of the angle was masked with tape, and the center of the total length was located and marked. A horizontal 2.0-centimeter grid, which began with 50.0 centimeters at the center and used numerically increasing and decreasing intervals to the opposite sides of the center was established. The angle was elevated above and centered

L9543

Fig. 8. Wet gage core before its installation in soil.

over the diagonals of the soil container. The angle was elevated so as not to interfere with the crater lip which would form during cratering.

The depth gage was a two-part device which consisted of a brass rod and tube. It was fabricated so that only the tens units were obtained from the brass rod while the units and decimals were obtained from an adjustable vernier (Fig. 9).

The 20.0-centimeter-long vernier was made from a 3/16-inch-diameter brass tube. An 11.0-centimeter longitudinal slot was milled through the center portion of the tube, and the edges of this slot were scribed so as to provide a 10.0-centimeter scale subdivide every 0.1 centimeter. The brass rod's zero division was located so that it would match the zero division on the vernier scale only when the lower ends of both the brass rod and the vernier tube matched. In this way, the vernier could be positioned against the reference plane; thus, the rod would drop into the crater and the depth would be determined by first reading the tens units on

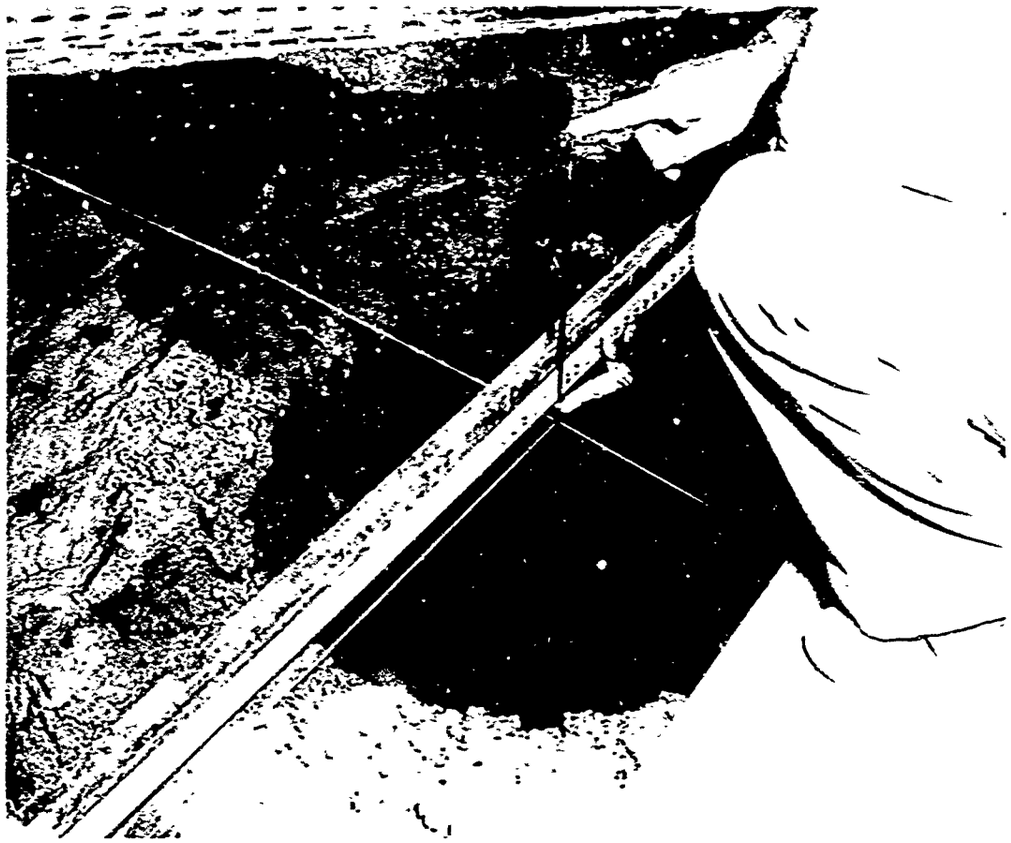

L9510

Fig. 9. Depth gage and steel angle used in measuring craters.

the rod, and then the units and decimal dimension would be obtained from the vernier.

When the soil, the gages, and the T1 target preparations were completed, the reference plane was positioned along a diagonal, and the 50.0-centimeter division was plumbed directly over the intersection of both diagonals. This located the center of the explosive charge and the gages. By means of the reference plane and the depth gage, the predetonation elevation of the soil medium was established along the 2.0-centimeter interval of both diagonals. The wooden core (the cardboard in the wet soil medium) was removed, and the dimensions to the top of the T1 target were recorded; thus, definite fixes were established on the locations of not only the explosive charge and the T1 target, but also all the emplaced gages.

The charge was placed in the shaft left by the wooden core and positioned directly over the T1 target. The soil medium of the particular test was carefully stemmed over the charge and the T1 target. The coaxial leads from the gages were then connected tc the dynamic gage circuit, and this entire circuit was connected to the oscilloscope. The T1 target leg wires were connected to the input terminals of a time delay generator (Model 20, Electronic Aids, Inc.) with the time delay set at zero. The delayed output terminal was then connected to the external trigger of the scopes used. The time delay generator was used only as a high-voltage source to trigger the scopes once the T1 target closed. Oscilloscope cameras were used to record the transition times with each detonation (Fig. 10).

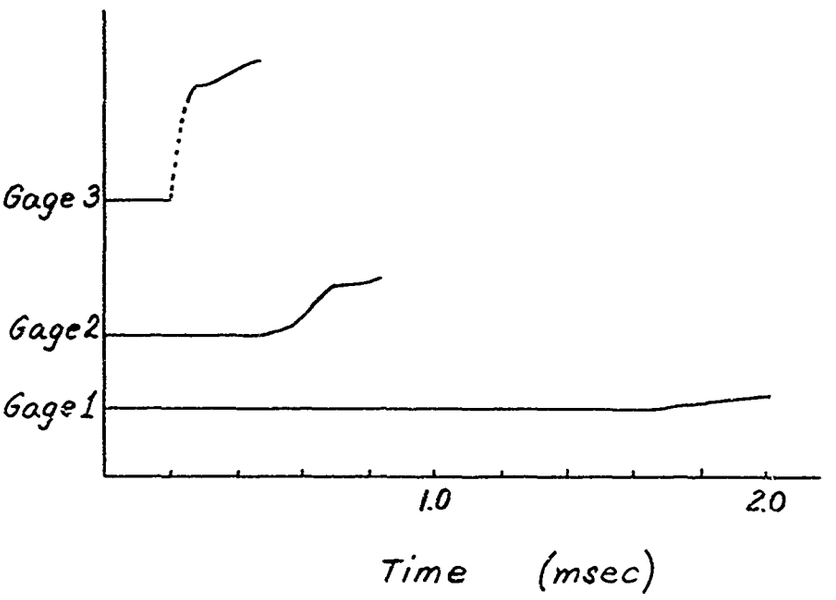

Fig. 10. Time-of-arrival oscilloscope traces obtained with strain gages.

Apparent crater measurements were taken immediately after the detonation. The procedure outlined here was employed to establish the predetonation elevation. True crater dimensions were recorded following the careful removal of all the loose soil medium from the crater.

Residual displacements of the gages were obtained by carefully removing the soil media at a given distance away from the original vertical plane of the gages and carefully shaving into this vertical plane until the gage locations were disclosed. The normal dimensions were then taken from the center of the reference plane to the gages as before.

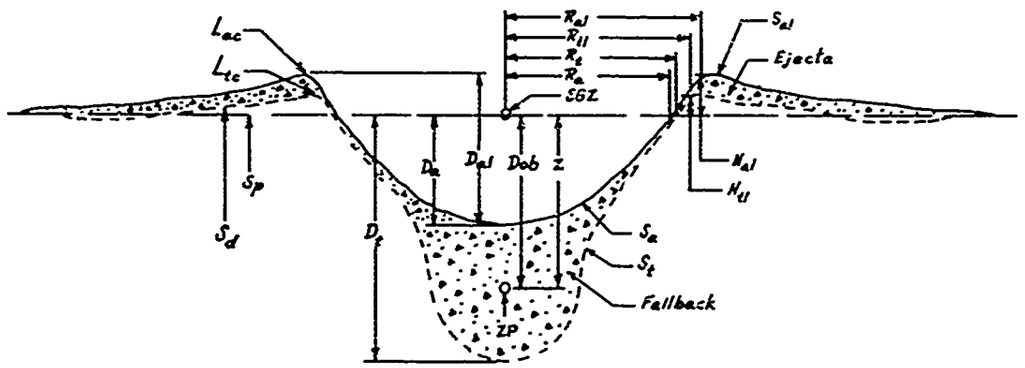

D_a..... Maximum depth of apparent crater below preshot ground surface measured normal to preshot ground surface.

D_{al}..... Depth of apparent crater below average apparent crater lip crest elevation.

Dob..... Normal depth of burst (measured normal to preshot ground surface).

D_t..... Maximum depth of true crater below preshot ground surface.

Ejecta.... Material above and/or beyond the true crater includes: (1) Foldback; (2) breccia--ballastic trajectory; (3) dust--aerosol transport, and the like.

Fallback.. Material fallen inside true crater includes: (1) Slide blocks; (2) breccia and stratified fallback--ballastic trajectory; (3) dust-aerosol transport; (4) talus; and the like.

H_{al}..... Apparent crater lip crest height above preshot ground surface.

H_{tl}..... True crater lip crest height above preshot ground surface.

L_{ac}..... Apparent crater lip crest.

L_{tc}..... True crater lip crest.

R_a..... Radius of apparent crater measured on preshot ground surface.

R_{al}..... Radius of apparent lip crest to center.

R_t..... Radius of true crater measured on preshot ground surface.

R_{tl}..... Radius of true lip crest to center.

S_a.....Apparent crater surface, for example, rock-air or rubble-air interface.

Sal..... Apparent lip surface.

SGZ..... Surface ground zero.

S_d.....Displaced ground surface.

S_p.....Preshot ground surface.

S_t..... True crater surface, for example, rock-air or rock rubble interface.

V_a.....Volume of apparent crater below preshot ground surface.

V_t..... Volume of true crater below preshot ground surface.

Z..... Vertical depth of burst (equivalent to Dob when crater is formed on a horizontal surface.)

ZP..... Zero point--effective center of explosion energy.

Fig. 11. Crater nomenclature.

B. TABULATED TEST DATA

9. Crater Nomenclature. The recorded measurements were tabulated and are presented in the following paragraphs. Figure 11 illustrates and defines the crater nomenclature used in the remainder of the report.

10. Crater Depth and Diameter Dimensions. Tables I and II present the actual scaled data for the true and apparent crater depths and diameters in the media having 10.6-percent and 21.0-percent soil moisture contents, respectively.

11. Remaining Crater Dimensions. Tables III and IV provide the remainder of the apparent and true crater dimensions obtained.

12. Crater Volumes. Table V provides the calculated apparent and true volumes for the medium with a soil moisture content of 10.6 percent, and Table VI provides the identical information for the medium with a soil moisture content of 21.0 percent.

13. Soil Property Data. Table VII gives the results from the sieve analysis of the samples of soil media obtained during the entire tests.

14. Soil Characteristics Data. Tables VIII and IX provide all the soil characteristics data collected to date.

15. Time-of-Arrival Data. The values shown in Tables X and XI were obtained from the oscilloscope traces such as the one shown in Fig. 10. The transient times between gages were obtained by measuring to the beginning of the voltage change.

16. Gage Displacement Data. The results of the gage displacement measurements are shown in Tables XII and XIII for the two soil media.

III. DISCUSSION

17. Adequacy of Methods and Equipment. The differences that are obtained in the crater parameters as a direct result of soil moisture content within the plastic index of the soil were successfully demonstrated in this investigation. Although difficulties in handling the plastic media and variance in soil consistency were encountered, they did not detract from the comparative analysis of this investigation. The methods and equipment used to determine and obtain the desired moisture contents, densities, gage

Table I. Crater Measurements for Soil Moisture Content of 10.6 Percent

Dob		D_t		$2R_t$		D_a		$2R_a$		$Dob/W^{1/3} \cdot 12$	$D_t/W^{1/3} \cdot 12$	$R_t/W^{1/3} \cdot 12$
(cm)	(in.)	(cm)	(in.)	(cm)	(in.)	(cm)	(in.)	(cm)	(in.)			
0.0	0.00	9.5	3.74	40.9	16.1	7.3	2.9	32.5	12.8	0.0	0.77	1.66
0.0	0.00	9.7	3.82	37.0	14.6	7.0	2.8	28.7	11.3	0.0	0.79	1.50
5.5	2.17	14.7	5.79	48.5	19.1	7.6	3.0	32.9	12.9	0.44	1.20	1.97
5.5	2.17	15.1	5.95	51.2	20.1	9.4	3.7	45.0	17.7	0.44	1.23	2.07
10.4	4.09	22.8	8.97	60.0	23.7	5.2	2.1	36.1	14.2	0.83	1.85	2.44
10.9	4.29	22.8	8.97	65.9	25.9	7.2	2.8	49.3	19.4	0.89	1.85	2.67
18.6	7.33	31.1	12.2	71.4	28.1	-4.0	-1.6	0.0	0.0	1.51	2.52	2.90
18.8	7.36	29.1	11.4	72.7	28.6	-5.5	-2.2	0.0	0.0	1.52	2.35	2.95
60.0	23.6	78.8	31.0	26.5	10.4	-	-	-	-	4.86	6.4	1.07

Note: Hyphens signify that no data were taken.

Table II. Crater Measurements for Soil Moisture Content of 21.0 Percent

Dob		D_t		$2R_t$		D_a		$2R_a$		$Dob/W^{1/3} \cdot 12$	$D_tW^{1/3} \cdot 12$	$R_t/W^{1/3} \cdot 12$
(cm)	(in.)	(cm)	(in.)	(cm)	(in.)	(cm)	(in.)	(cm)	(in.)			
0.0	0.00	21.9	8.62	49.3	19.4	21.9	8.62	49.3	19.4	0.0	1.78	2.00
"	"	25.7	10.1	47.3	18.6	25.7	10.1	47.3	18.6	"	2.08	1.92
"	"	23.6	9.29	50.8	20.1	23.6	9.29	50.8	20.1	"	1.91	2.07
5.3	2.09	31.9	12.6	72.0	28.3	31.9	12.6	72.0	28.3	0.43	2.59	2.92
5.9	2.32	35.8	14.1	71.2	28.0	35.8	14.1	71.2	28.0	0.48	2.91	2.89
12.2	4.81	40.2	15.8	70.0	27.6	40.2	15.8	70.0	27.6	0.99	3.26	2.85
9.3	3.66	35.8	14.1	74.6	29.4	35.8	14.1	74.6	29.4	0.75	2.91	3.03
18.8	7.40	42.9	16.9	63.0	24.8	41.4	16.3	63.0	24.8	1.52	3.49	2.56
19.5	7.67	46.5	18.3	66.1	26.1	41.7	16.4	66.1	26.1	1.58	3.77	2.69
60.0	23.6	85.5	33.7	36.6	14.4	85.5	33.7	36.6	14.4	4.86	6.95	1.48

Table III. Other Crater Measurements for Soil Moisture Content of 10.6 Percent

Dob		$2R_{t\ell}$		$2R_{a\ell}$		$H_{t\ell}$		$H_{a\ell}$		$D_t + H_{t\ell}$		$D_a + H_{a\ell}$		$Dob/W^{1/3}$
(cm)	(in.)	(cm)	(in.)	(cm)	(in.)	(cm)	(in.)	(cm)	(in.)	(cm)	(in.)	(cm)	(in.)	
0.0	0.00	43.0	16.9	41.7	16.4	0.7	0.27	1.3	0.51	10.2	4.01	8.6	3.38	0.0
0.0	0.00	37.1	14.6	32.9	12.9	0.0	0.00	0.8	0.31	9.7	3.82	7.8	3.07	0.0
5.5	2.17	51.8	20.4	44.1	17.4	0.6	0.23	1.8	0.71	15.3	6.03	9.4	3.70	0.44
5.5	2.17	52.2	20.5	49.3	19.4	0.4	0.16	0.9	0.35	15.5	6.10	10.3	4.06	0.44
10.4	4.09	64.7	25.5	44.6	17.5	0.8	0.31	2.2	0.87	23.6	9.3	7.4	2.91	0.83
10.9	4.29	74.8	29.5	55.9	22.0	0.0	0.00	1.7	0.67	22.8	8.98	8.9	3.51	0.89
18.6	7.33	74.0	29.1	0.0	0.0	1.7	0.67	2.7	1.06	32.8	12.9	0.0	0.0	1.51
18.8	7.36	79.0	31.1	0.0	0.0	0.8	0.31	2.5	0.98	29.9	11.8	0.0	0.0	1.52
60.0	23.60	N/A		N/A		N/A		N/A		N/A		N/A		4.86

Note: N/A denotes data are not applicable.

Table IV. Other Crater Measurements for Soil Moisture Content of 21.0 Percent

Dob		$2R_{t\ell}$		$2R_{a\ell}$		$H_{t\ell}$		$H_{a\ell}$		$D_t + H_{t\ell}$		$D_a + H_{a\ell}$		$Dob/W^{1/3}$
(cm)	(in.)	(cm)	(in.)	(cm)	(in.)	(cm)	(in.)	(cm)	(in.)	(cm)	(in.)	(cm)	(in.)	
0.0	0.0	56.1	22.1	56.1	22.1	10.4	4.1	10.4	4.1	32.3	12.7	32.3	12.7	0.0
"	"	52.0	20.5	52.0	20.5	6.4	2.5	6.4	2.5	32.1	12.6	32.1	12.6	"
"	"	62.1	24.5	62.1	24.5	5.4	2.1	5.4	2.1	29.0	11.4	29.0	11.4	"
5.3	2.09	84.0	33.1	84.0	33.1	7.0	2.7	7.0	2.7	38.9	15.3	38.9	15.3	0.43
5.9	2.32	78.3	30.9	78.3	30.9	10.1	3.9	10.1	3.9	45.9	18.0	45.9	18.0	0.48
12.2	4.81	75.2	29.5	75.2	29.5	8.5	3.3	8.5	3.3	48.7	19.1	48.7	19.1	0.99
9.3	3.66	75.3	29.7	75.3	29.7	6.5	2.5	6.5	2.5	42.3	16.6	42.3	16.6	0.75
18.8	7.40	85.7	33.8	85.7	33.8	7.0	2.7	7.0	2.7	49.9	19.6	48.4	19.1	1.52
19.5	7.67	78.5	30.9	78.5	30.9	10.5	4.1	10.5	4.1	57.0	22.5	52.2	20.5	1.58
60.0	23.60	N/A		N/A		N/A		N/A		N/A		N/A		4.86

Note: N/A denotes data are not applicable.

Table V. Apparent and True Crater Volumes for Soil Moisture Content of 10.6 Percent

Dob (cm)	Dob (in.)	Apparent Volume (cc)	True Volume (cc)	Dob/$W^{1/3}$
0.0	0.00	1,248	3,990	0.0
0.0	0.00	1,738	3,990	0.0
5.5	2.17	2,510	10,550	0.44
5.5	2.17	4,820	12,170	0.44
10.4	4.09	3,010	49,700	0.83
10.9	4.29	5,850	59,500	0.89
18.6	7.33	0.0	62,300	1.51
18.8	7.36	0.0	49,400	1.52
60.0	23.60	-	-	4.86

Note: Hyphens signify that no data were taken.

Table VI. Apparent and True Crater Volumes for Soil Moisture Content of 21.0 Percent

Dob (cm)	Dob (in.)	Apparent Volume (cc)	True Volume (cc)	Dob/$W^{1/3}$
0.0	0.00	No Apparent Vol.	25,700	0.0
"	"	" " "	28,600	"
"	"	" " "	30,700	"
5.3	2.09	" " "	77,400	0.43
5.9	2.32	" " "	88,800	0.48
12.2	4.81	" " "	105,700	0.99
9.3	3.66	" " "	86,900	0.75
18.8	7.40	88,200	90,200	1.52
19.5	7.67	103,100	111,900	1.58
60.0	23.60	-	-	4.86

Note: Hyphens signify that no data were taken.

Table VII. Sieve Analysis of Samples of Soil Media

Screen No.	Dob (cm)																
	0.0	0.0	5.5	5.5	10.4	10.9	18.6	18.8	0.0	0.0	0.0	5.3	5.9	12.2	9.3	18.8	19.5
	Percentage Passing Screen																
4	100	100	100	100		100	100	100	100	100		100	100	100	100	100	100
10	97.5	97.0	98.0	88.7		95.3	97.5	97.5	98.0	99.5		99.0	98.7	98.0	99.3	98.3	99.3
40	86.0	79.0	85.5	59.5		68.3	87.5	89.0	72.1	74.3		67.8	72.4	74.5	79.3	64.5	57.7
60	75.3	61.0	74.0	48.2		45.9	76.0	76.0	52.9	57.0		53.2	56.6	59.8	64.3	48.8	41.0
100	64.8	33.4	62.5	38.8		23.7	63.5	61.0	40.8	45.0		43.5	46.9	48.0	54.3	38.5	31.7
200	54.3	9.4	52.5	29.0		13.8	51.0	44.0	32.3	36.5		37.0	40.2	40.5	46.9	32.0	26.3

Table VIII. Soil Characteristics for Soil Moisture Content of 10.6 Percent

Lob (cm)	Dob / W^1/3	Moisture Content (%)	Plastic Limit (%)	Liquid Limit (%)	Sieve Analysis (% Sand)	Sieve Analysis (% Fines)	Soil Density Wet (lb/cu ft)	Soil Density Dry (lb/cu ft)	Shear Strength	Cohesive Strength	Void Ratio	Angle of Int Friction	Optimum Moisture Content
0.0	0.00	10.7	18.0	21.0	45.7	54.3	105.5	96.0					
0.0	0.00	9.8	16.0	19.0	55.0	45.0	100.9	93.0					
5.5	0.44	10.3	16.0	21.0	50.0	50.0	116.2	106.0					
5.5	0.44	10.4	17.0	21.0	71.0	29.0	114.6	106.0					
10.4	0.83	11.1	-	-	-	-	110.3	101.7					
10.9	0.89	11.5	19.0	25.0	86.2	13.8	-	-					
18.6	1.51	10.2	17.0	22.0	49.0	51.0	107.8	98.4					
18.8	1.52	10.9	17.0	22.0	56.0	44.0	113.0	103.8					
60.0	4.86	-	-	-	-	-	-	-					

Note: Hyphens signify that no data were taken.

Table IX. Soil Characteristics for Soil Moisture Content of 21.0 Percent

Dob (cm)	$\frac{Dob}{W^{1/3}}$	Moisture Content (%)	Plastic Limit (%)	Liquid Limit (%)	Sieve Analysis (% Sand)	Sieve Analysis (% Fines)	Soil Density Wet (lb, cu ft)	Soil Density Dry (lb/cu ft)	Shear Strength	Cohesive Strength	Void Ratio	Angle of Int Friction	Optimum Moisture Content
0.0	0.00	21.2	17.0	20.0	69.2	30.8	-	-					
"	"	21.0	17.0	21.0	64.0	36.0	129.8	107.7					
"	"	-	-	-	-	-	-	-					
5.3	0.43	20.3	18.0	21.0	64.1	35.9	121.5	100.7					
5.9	0.48	22.2	18.0	24.0	60.5	39.5	-	-					
12.2	0.99	21.2	-	-	60.2	39.8	136.7	114.0					
9.3	0.75	20.2	18.0	21.0	53.9	46.1	124.1	103.3					
18.8	1.52	20.6	17.0	23.0	68.0	32.0	112.3	94.1					
19.5	1.58	21.5	18.0	20.0	75.8	24.2	-	-					
60.0	4.86	-	-	-	-	-	-	-					

Note: Hyphens signify that no data were taken.

Table X. Time of Arrival for Soil Moisture Content of 10.6 Percent

Dob (cm)	Dob / $W^{1/3}$	Distance between T1 Target and SR-4 Strain Gage / Time of Arrival of Shock Front at SR-4 Strain Gage							
		d_4 (cm)	t_4 (msec)	d_3 (cm)	t_3 (msec)	d_2 (cm)	t_2 (msec)	d_1 (cm)	t_1 (msec)
0.0	0.00	4.9	0.010	10.0	0.17	19.8	0.58	30.0	1.10
0.0	0.00	7.5	0.070	12.5	0.27	22.3	-	41.1	-
5.5	0.44	5.2	-	14.8	-	24.8	-	34.8	-
5.5	0.44	5.4	0.015	9.9	0.16	20.6	-	31.2	-
10.4	0.83	-	-	10.5	0.18	20.5	0.56	31.5	0.90
10.9	0.89	5.0	0.015	10.0	0.13	20.0	0.56	30.0	0.94
18.6	1.51	5.1	0.020	9.8	0.16	15.1	0.48	25.1	0.65
18.8	1.52	6.0	0.050	9.9	-	15.6	0.34	-	-
60.0	4.86	-	-	-	-	-	-	-	-

Note: Hyphens signify that no data were taken.

Table XI. Time of Arrival for Soil Moisture Content of 21.0 Percent

Dob (cm)	Dob / $W^{1/3}$	Distance between T1 Target and SR-4 Strain Gage / Time of Arrival of Shock Front at SR-4 Strain Gage							
		d_4 (cm)	t_4 (msec)	d_3 (cm)	t_3 (msec)	d_2 (cm)	t_2 (msec)	d_1 (cm)	t_1 (msec)
0.0	0.00	4.7	-	9.7	-	19.4	-	28.0	-
"	"	5.1	0.015	10.6	0.05	19.6	0.28	29.4	0.41
"	"	-	-	-	-	-	-	-	-
5.3	0.43	5.5	0.055	10.6	0.06	15.0	-	30.9	-
5.9	0.48	4.5	0.020	10.1	0.07	15.2	0.14	30.2	0.59
12.2	0.99	6.4	0.025	11.2	0.07	15.4	0.13	25.5	0.30
9.3	0.75	7.0	0.026	10.0	0.072	21.4	0.16	34.0	0.48
18.8	1.52	4.8	-	10.6	-	15.3	-	24.5	-
19.5	1.58	8.2	0.030	13.5	0.07	18.5	0.17	27.8	0.30
60.0	4.86	-	-	-	-	-	-	-	-

Note: Hyphens signify that no data were taken.

Table XII. Net Gage Movement for Soil Moisture Content of 10.6 Percent

Dob (cm)	Dob / $W^{1/3}$	Original Distance between Gage and Bottom of Charge				Net Gage Movement			
		Gage - #4 (cm)	#3 (cm)	#2 (cm)	#1 (cm)	Gage - #4 (cm)	#3 (cm)	#2 (cm)	#1 (cm)
0.0	0.00	4.9	10.0	19.8	30.0	3.4	1.4	0.0	0.2
0.0	0.00	7.8	12.8	22.6	41.4	1.5	0.2	-1.0	-1.3
5.5	0.44	5.5	15.1	25.1	35.1	3.2	-2.7	-	-
5.5	0.44	5.7	10.2	20.9	31.5	0.3	1.5	0.0	0.0
10.4	0.83	-	10.8	20.8	31.8	-	1.1	0.0	0.0
10.9	0.89	-	-	20.3	30.3	-	-	1.1	-0.9
18.6	1.51	5.4	10.1	15.4	25.4	1.0	1.4	0.9	0.0
18.8	1.52	-	10.2	15.9	-	-	3.1	1.9	-
60.0	4.86	-	-	-	-	-	-	-	-

Note: Hyphens signify that no data were taken.

Table XIII. Net Gage Movement for Soil Moisture Content of 21.0 Percent

Dob (cm)	Dob / $W^{1/3}$	Original Distance between Gage and Bottom of Charge				Net Gage Movement			
		Gage - #4 (cm)	#3 (cm)	#2 (cm)	#1 (cm)	Gage - #4 (cm)	#3 (cm)	#2 (cm)	#1 (cm)
0.0	0.00	5.0	10.0	19.7	28.3	15.9	11.6	6.3	4.4
"	"	5.4	10.9	19.9	29.7	13.9	8.4	4.0	1.2
"	"	-	-	-	-	-	-	-	-
5.3	0.43	5.8	10.9	15.3	31.2	21.6	13.9	11.9	6.8
5.9	0.48	4.8	10.4	15.5	30.5	23.4	16.4	15.5	6.9
12.2	0.99	6.7	11.5	15.7	25.8	18.5	14.3	10.1	4.1
9.3	0.75	7.0	10.0	21.4	34.0	17.7	17.5	8.4	4.0
18.8	1.52	5.1	10.9	15.6	24.8	13.5	9.7	7.2	5.2
19.5	1.58	8.5	13.8	18.8	28.1	15.6	12.5	8.4	2.9
60.0	4.86	-	-	-	-	-	-	-	-

Note: Hyphens signify that no data were taken.

measurements, and crater measurements proved to be more than adequate for this investigation.

The crater data obtained were analyzed to determine the functional relationship between the variables for each moisture content and are presented graphically using a least square curve fitting technique. It is pertinent to realize that no logical conclusions can be derived from this graphical or analytical presentation beyond the experimental data points.

18. Crater Profiles. The immediately apparent contrast in crater formations of wet and dry media was the negligible amount of fallback material contained in wet soil craters. In only the two deeper depths of burst, 18.8 and 19.5 centimeters, was there any appreciable amount of fallback as is evident in the plotted crater profiles (Appendix B) and in Figs. 12, which shows the crater produced at the depth of burst of 9.3 centimeters. Consequently, discussions are directed toward a comparison of the true dimensions of the wet soil medium and the apparent and true dimensions in the dry soil medium.

True crater profiles in the dry and wet soil media exhibited distinctly different forms. In the dry soil medium, craters were divided into two distinctive upper and lower formations. The upper formation begins at or just below the center of the charge and exhibits an almost horizontal shear plane for some length. Then, a gradual or steep side slope which depends upon the depth of burst begins. The lower formation commences at the horizontal shear plane, extends beneath the charge center, and forms a well-compacted, charred, hemispherical shape. The hemispherical surface is also characterized by radial cracks which form segmented dense chunks of earth. truncated pyramids that have their vertices located at the center of the charge (Appendix B, Exhibit 1).

The nearly regular and symmetrical profiles in the wet soil medium resembled a large diameter paraboloid, the entire charred, well-compacted surface of which was characterized by the deeper radial cracks and larger segmented dense chunks of wet soil medium. Near vertical cavity sides and the much larger true crater lip are also distinguishing features of the crater formation in the wet soil medium.

When profiles in the dry and wet media are compared, the pattern of fallback provides another contrast in fundamental behavior. The small soil clods of the dry soil medium were ejected over a large area, whereas the clods of the wet soil medium were extremely large and scattered over a comparatively small area near the periphery of the crater lip.

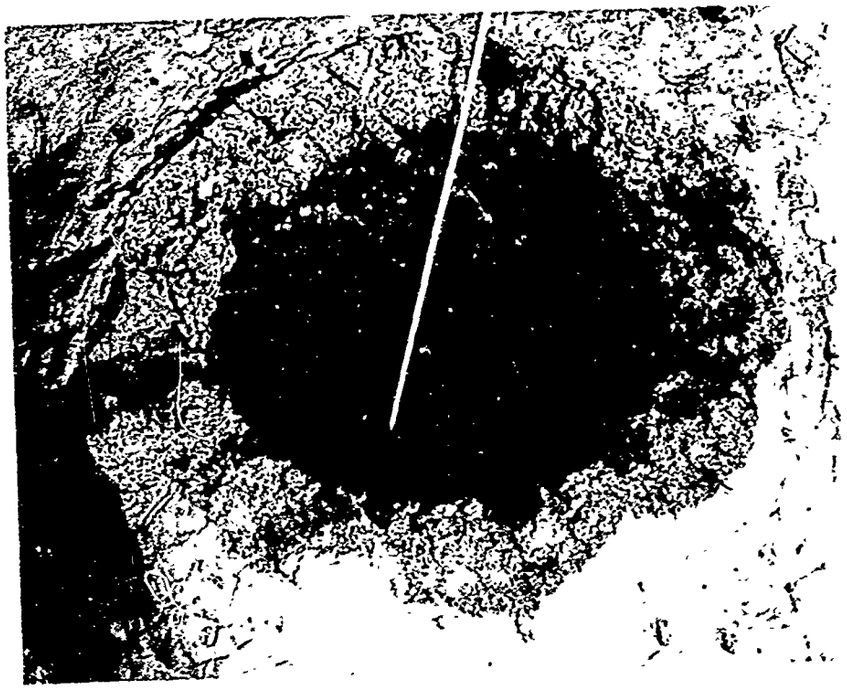

L9508

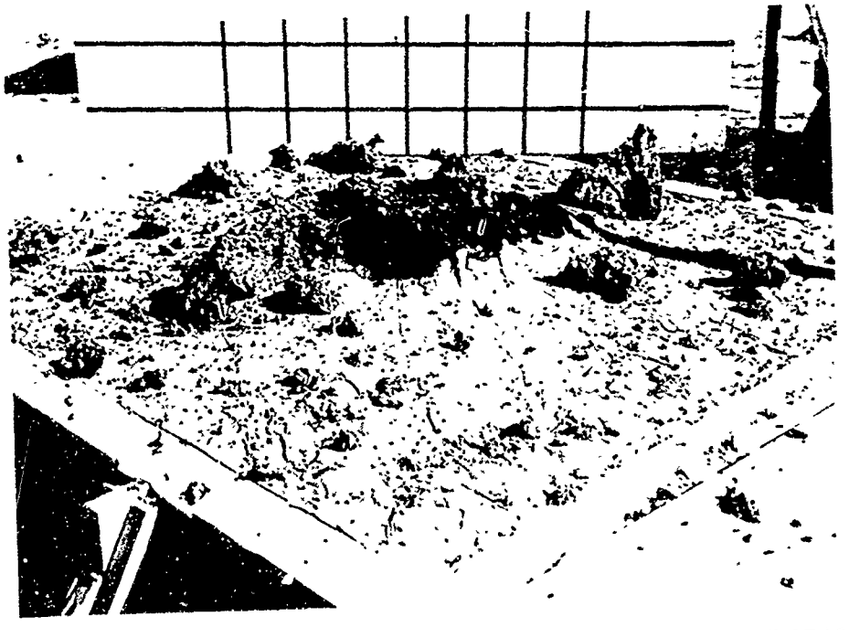

L8741

Fig. 12. Crater produced at depth of burst of 9.3 cm. Top: Profile obtained in wet soil medium. Bottom: Large clods and debris pattern obtained in same medium.

The tendency of steep side slopes to slide and the large fracture cracks to consolidate after the detonations resulted in crater profile changes with time in the wet soil medium (Fig. 12). Three of the first detonations were measured immediately after explosion and approximately 2 hours later. The procedure revealed that some changes in crater profiles took place; this amounted to a maximum decrease of 2 percent in depth of any point on the profile.

Panama Canal (4) and Camp Cooke (5) large-scale cratering tests, conducted in 1947 and 1953, respectively, were used to critically examine the basic crater profiles obtained in tests in a wet medium. These large-scale cratering tests were conducted in soils that possessed similar soil characteristics of plasticity and moisture content to those used in the experiments. Examination revealed the crater formation phenomenon of negligible fallback, which resulted in apparent and true crater profiles being practically identical, parabolic crater contours, and a congested debris pattern of large clods centered about the crater lip area. The Panama Canal report is quoted here, and Figs. 13 and 14 show these results:

> Generally the sides of the crater near the ground surface showed no evidence of debris such as is characteristic of apparent craters. The outlines of the apparent and true crater at the ground surface in marine muck are taken as being the same. (4)

One can readily visualize combat areas where this beneficial phenomenon (if it occurs while the Atomic Demolitions Munitions are being used), will result in more effective obstacles as a result of the increased crater dimensions, debris size, and residual radiation. Also, because of the possible lack of fallback, this increased residual radiation, above the predicted amount, could prove to be an adversity to friendly troop maneuvers and safety considerations for relatively long periods of time. An identical situation may occur during peaceful use of nuclear explosives in these types of media.

19. Crater Diameters. Variation in the true and apparent crater diameters obtained in the two media as a function of depth of burst are shown in Fig. 15. The equations of these curves are as follows:

$$2R_t = -0.19x^2 + 4.41x + 49.94 \text{ for the wet medium} \quad (1)$$

$$2R_t = -0.4x^2 + 2.64x + 38.35 \text{ for the dry medium} \quad (2)$$

$$2R_a = -0.31x^2 + 4.19x + 29.15 \text{ for the dry medium} \quad (3)$$

M12568

M12569

Fig. 13. Results of large-scale cratering tests conducted at Panama Canal. Top: Profile obtained in marine muck from 8-lb TNT explosion. Bottom: Large clods and debris pattern of same crater.

M12571

M12570

Fig. 14. Crater phenomenon at Panama Canal. Top: Profile obtained in marine muck from 25-lb TNT explosion. Bottom: Large clods and debris pattern of same crater.

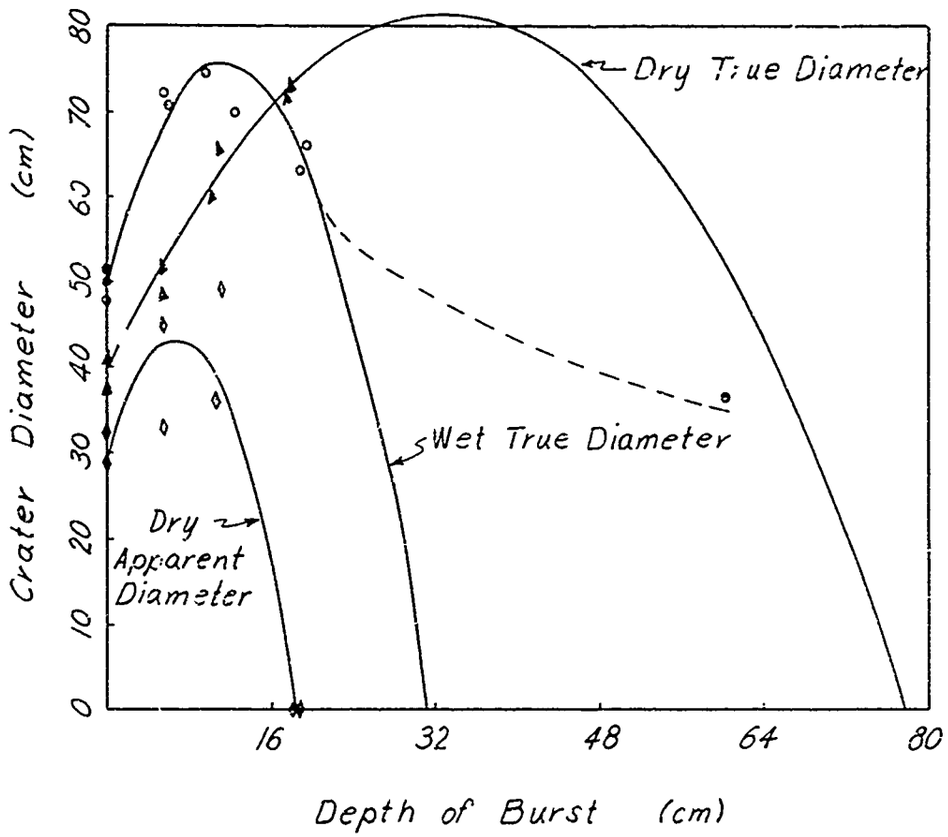

Fig. 15. Depth of burst vs crater diameter.

When reference is made to the true diameter curve in the wet medium, it is important to realize that as plotted it is a combination of both the true diameters obtained and the possible behavior of the apparent crater diameter. The actual true diameter curve would follow the solid line curve to the last experimental observation at 19.5 centimeters and then proceed along the indicated dashed line to the camouflet diameter.

True diameters in the wet medium exceed those in the dry medium by a factor of 1.3 or greater until the depth of burst exceeds 16.0 centimeters, at which point the true diameters are the same in both media. Thereafter, diameters of the dry medium exceed those of the wet medium and approach a predicted optimum of 81.9 centimeters at a depth of burst of 33.0 centimeters. Optimum true diameters in both media are approximately equivalent, but the dry medium appears to reach this optimum diameter at a depth of burst three times greater than that of the wet medium.

Tentatively, it appears that considerably less emplacement effort will be required to obtain greater or equivalent true diameters in the wet medium.

Because the fallback is negligible in the wet medium the comparison of the apparent crater diameters in the dry medium against the true diameters in the wet medium reveals the real significance of moisture content. This comparison reveals that the true crater diameters of the wet medium exceed the apparent diameters of the dry medium by a factor which varies from 1.7 to even larger values. These values must then be considered when one determines the enlarged widths of obstacles or effective excavations that might be obtained in the wet medium.

Experimental data and variables involved were used in a Regression and Correlation program to develop the following equation

$$2R_t = 5.25(\text{Dob}) - 0.125(\text{Dob})^2 + 1.669(M_c) - 0.101(\text{Dob})(M_c) + 17.19 \quad (4)$$

where M_c is moisture content of the soil expressed as percent by weight. The order in which independent variables Dob, $(\text{Dob})^2$, M_c, and $(\text{Dob})(M_c)$ are listed in the equation indicates their relative importance. It is estimated that 89.3 percent of the variation in $2R_t$ is accounted for by variations of these independent variables. Appendix C, Table XIV, gives the estimated percentage of variation in $2R_t$, that is accounted for by each variable.

20. Crater Depths. Figure 16 depicts the linear behavior of the true crater depth versus depth of burst for each medium and the functional relationships are given by

$$D_t = 1.01x + 25.77 \text{ for the wet medium} \quad (5)$$

$$D_t = 1.15x + 9.32 \text{ for the dry medium} \quad (6)$$

A functional relationship between the apparent crater depth and the depth of burst for the dry medium is expressed by

$$D_a = -0.07x^2 + 0.63x + 7.12 \text{ for the dry medium} \quad (7)$$

and is graphically represented in this figure. Although an apparent crater depth for the wet medium is not shown here because of the lack of fallback, it is reasonable to assume that soon after the 19.0-centimeter observation considerable fallback would begin to enter the true crater. This will bring about an apparent crater depth which will deviate from the true crater depth relationship and proceed to a zero depth as indicated by the dashed line.

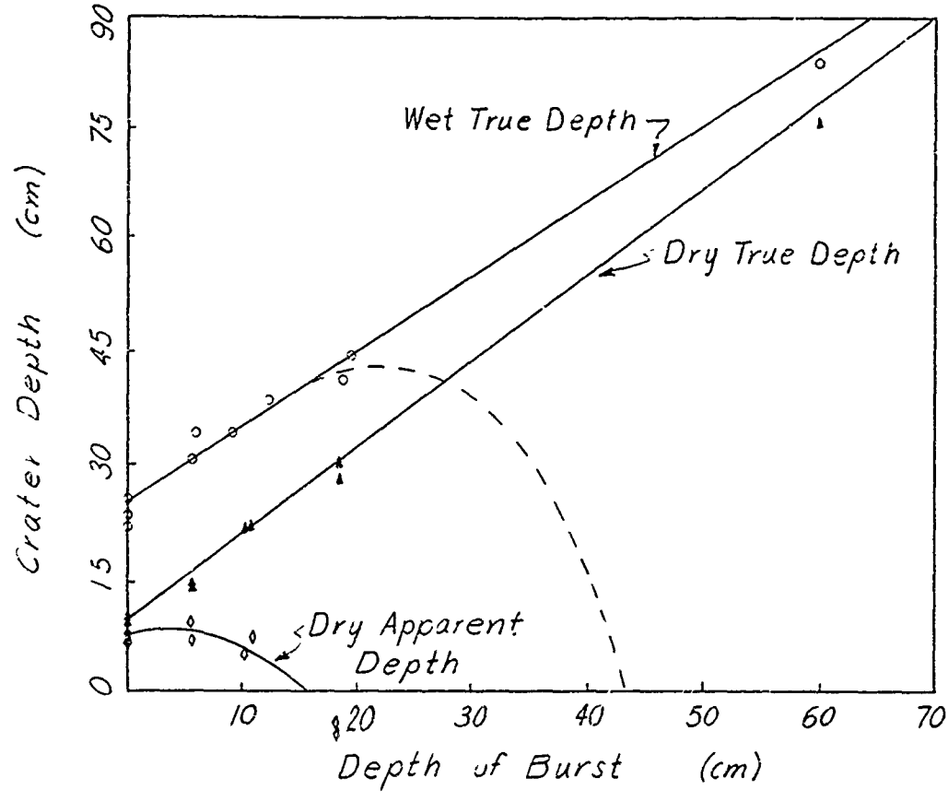

Fig. 16. Depth of burst vs crater depth.

True crater depth of the wet medium varies from 25.8 centimeters at the surface to 44.5 centimeters at a depth of burst of 18.5 centimeters. These wet true depths exceed the dry true depths by factors that vary from 2.8 to 1.5.

Again, the most revealing comparison is between the true depth of the wet medium and the apparent depth of the dry medium. Here, the true depth in the wet medium exceeds the apparent depth in the dry medium by 3.6 at zero depth of burst and continues to exceed the dry medium by even greater factors at all experimental observations. As a result of these larger true depths, the obstacles formed will be enhanced not only by the larger depths but also by the steep side slopes that are produced.

The following equation:

$$D_t = 1.303(\text{Dob}) + 1.581(M_c) - 0.014(\text{Dob})(M_c) - 7.44 \qquad (8)$$

was developed by the use of the Regression and Correlation program and estimates the true crater depths with variations in the depths of burst and the moisture content. The independent variables estimate 99.3 percent of the variations in the true crater depths with the predominant variable depth of burst estimating 85.6 percent of the total variation. Inclusion of moisture content increases the estimate to 98.8 percent (Appendix C, Table XIV).

21. Crater Volumes. It appears that all parameters of the crater formation are enhanced by the addition of water to this soil medium. The true crater volume was used as a measurement of the useful explosive energy imparted to the soil medium. It was found that the efficiency of the explosive energy coupling has increased considerably. Although soil mechanical properties may have been reduced and account for a portion of the increased volume, they cannot be expected to account for an approximate sevenfold increase in crater volumes. The Bass, Hawk, and Chabai (6) equation of state investigations on dry and water-saturated silica sand is evidence of the much improved energy coupling.

The experimental volume data, taken at 2.0-centimeter intervals, were used to calculate the volumes of the craters by the truncated cone method described by Dennis (7). The volume versus the depth of burst data were plotted and are shown in Fig. 17. Equations of the volume are:

$$V_t = -348.8x^2 + 10421.0x + 29550.4 \text{ for the wet medium} \quad (9)$$

$$V_t = -49.50x^3 + 1235.45x^2 - 3128.2x + 6102.3 \text{ for the dry medium} \quad (10)$$

$$V_a = -41.04x^2 + 698.08x + 1384.2 \text{ for the dry medium} \quad (11)$$

It is evident immediately that larger true crater volumes were produced in the wet medium when compared to the true crater volumes in the dry medium. At the surface, a sevenfold increase over the true dry volume is observed. It is interesting to note that the optimum true crater volume in the wet and dry media appear to be produced at the same depth of burst (Fig. 17), whereas the optimum true diameters are obtained at considerably different depths of burst (Fig. 15). An unexpected behavior of the true dry volume occurs between the surface detonation and a depth of burst of about 5.0 centimeters (Fig. 17). The volume increases gradually until it reaches a crucial depth of burst; thereafter, it increases readily to the optimum volume. Additional information bracketing the 5.0 centimeters depth of burst would determine a more precise behavior.

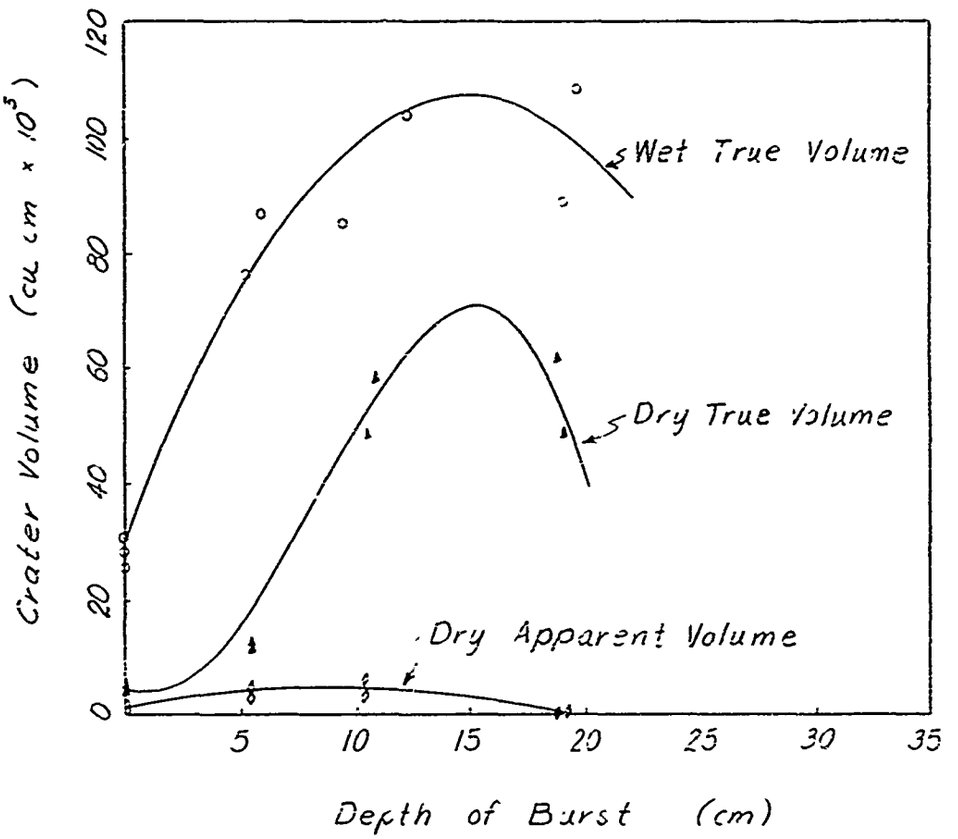

Fig. 17. Depth of burst vs cater volume.

In the preceding paragraphs, emphasis has been given to the comparative analysis between true crater dimensions of the wet medium compared to the apparent crater dimensions of the dry medium. This was done to demonstrate the enhanced obstacle and excavation craters that would be formed as a result of detonations in wet medium, the consistency of which approaches the plastic limit, without the additional effort of removing fallback material from the crater. It is readily seen that the apparent volume of the dry medium is insignificant compared to the true volume of the wet medium. Detonation at the surface in the wet medium yields a seventeenfold increase in volume over the dry medium, and when the volume in the dry medium is nonexistent the optimum volume in the wet medium has been reached.

The following equation

$$V_t = 8162.6(\text{Dob}) + 4317.8(M_c) - 244.98(\text{Dob})^2 - 55212.7 \qquad (12)$$

was developed by use of the Regression and Correlation program. Depth of burst, the predominating variable, explained an estimated 45.7 percent of the variation in volume. Inclusion of moisture content raised the level of explained variation to an estimated 83.5 percent. The level of explained variation in volume rose to an estimated 91.5 percent when depth of burst squared ($(Dob)^2$) was included.

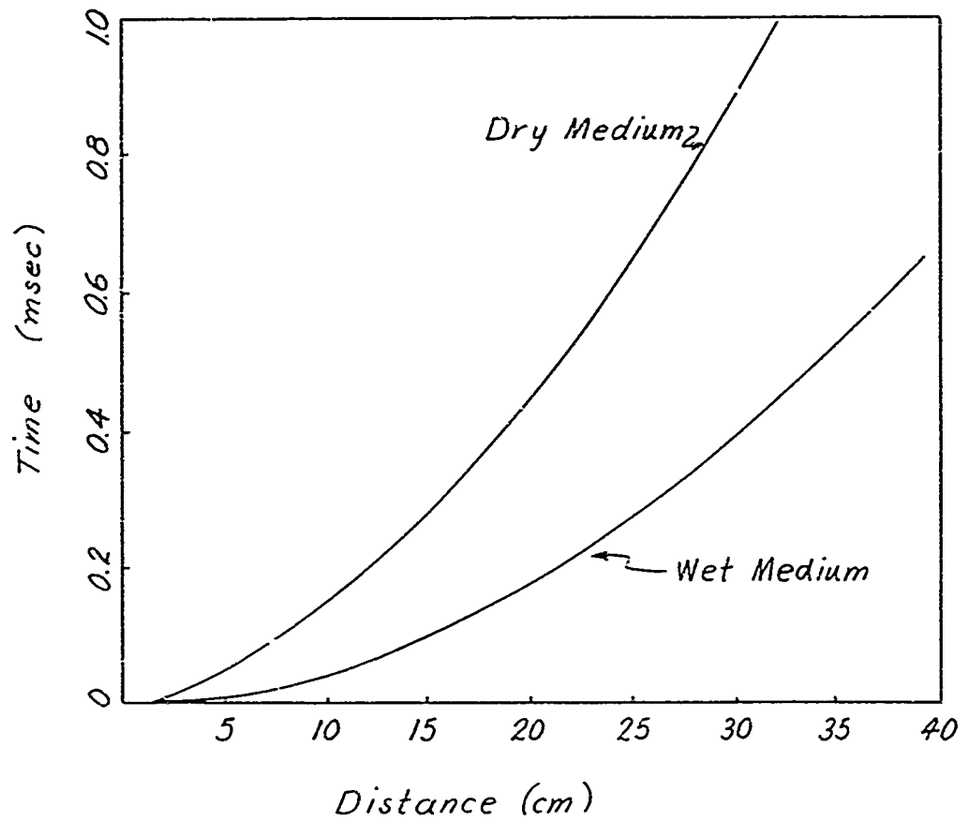

Fig. 18. Distance between center of charge and gage vs time of arrival.

22. Time-of-Arrival Data and Shock Velocities. The numerical curve-fitted time-of-arrival data for the two soil media are shown in Fig. 18 and are expressed by the following equations

$$t_a = 0.00041x^2 + 0.0005x - 0.00205 \text{ for the wet medium} \quad (13)$$

$$\text{and } t_a = 0.00069x^2 + 0.00904x - 0.01737 \text{ for the dry medium} \quad (14)$$

The time-of-arrival value at the C4 explosive-soil interface is an extrapolated value determined by the detonation velocity of the explosive. This

value, taken at 1.7 centimeters from the center of the explosive charge, was taken to be zero because the actual value was extremely small (nanoseconds) compared to the observed times (milliseconds).

After the resulting distance-time equations 13 and 14 obtained from the time-of-arrival data were differentiated, the shock velocities were determined in the two media. When it is known that the pressure-time profile behind the detonation front is very steep, the velocities of the shock in the soil media will attenuate quickly within a short distance past the C4-soil interface. Therefore, in the interval between the C4-soil interface and the first strain gage, approximately 5.0 centimeters, the most rapid attentuation occurs. For this reason, the extrapolation from 6.7 centimeters to 1.7 centimeters, zero length, does not follow the true attenuation, and the extrapolated shock velocities will be lower than the actual velocities at the C4-soil interface. Figure 19 depicts the shock velocity as a function of radius from charge. The measured and extrapolated values are shown as a solid line, and interpolated values are dashed lines. Attenuation in the dry medium is seen to be most drastic and appears to be less pronounced in the wet medium.

At the first experimental observation, the shock velocity is approximately 3 times greater in the wet medium and attenuates more rapidly than does that in the dry medium. At a radius of 25.0 centimeters, the factor is reduced to twice that of the dry medium and remains constant to the last observation of 43.0 centimeters. The shock velocity in the wet medium is greater than that in the dry medium; hence, it would be reasonable to assume that the associated pressures are also greater by a related factor.

The following time-of-arrival equation

$$t_a = 0.496(D) - 0.00207(D)(M_c) + 0.0107(M_c) + 0.000294(D)^2 - 0.255 \quad (15)$$

was developed by the Regression and Correlation programs and indicates the distance (D) namely, radius from the charge to be the most important variable, estimating 69.7 percent of the variation in the time-of-arrival data. Inclusion of the cross product term $(D)(M_c)$ raises the explanation to 94.3 percent of the variance in time of arrival. The level of explained variance rose to an estimated 95.7 percent when M_c and $(D)^2$ were included. Results of this analysis are presented in Appendix C, Table XIV.

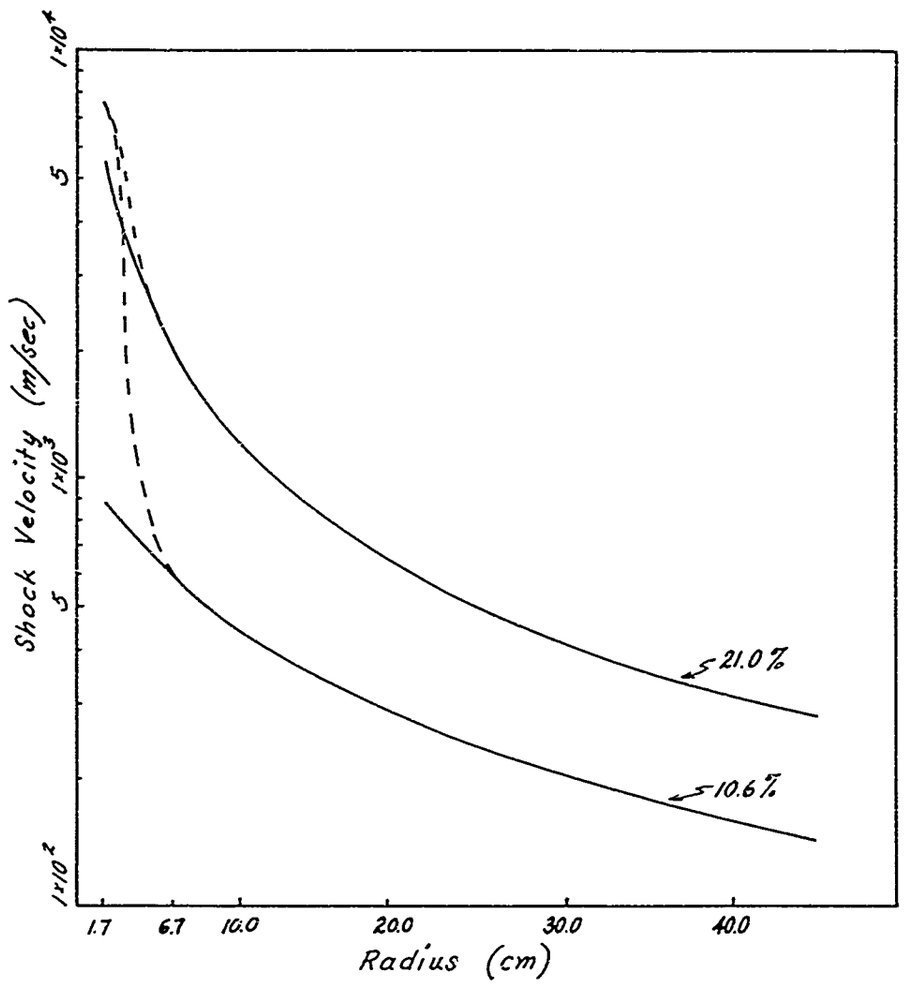

Fig. 19. Radius vs shock velocity.

23. Net Gage Displacements. The net gage displacements were treated in two ways: (1) A comparative analysis of the displacements obtained in the two media was made; and, (2) the displacements in each medium were then examined at selected depths of burst. The purpose was to determine whether depth of burst exerted significant influence on the locus, net displacement versus distance from the bottom of the charge.

The comparative analysis of net gage displacement (G_d) versus distance from the bottom of the charge is given by

$$G_d = 0.0168x^2 - 1.1565x + 23.85 \text{ for the wet medium} \quad (16)$$

and $$G_d = 0.0024x^2 - 0.1857x + 2.939 \text{ for the dry medium.} \quad (17)$$

The dry medium exhibits a near linear behavior when compared to the wet medium displacements. The displacements in the wet medium at the first observation of 5.0 centimeters exceed the dry medium displacement by approximately a factor of 9. At 21.5 centimeters the dry medium had practically zero displacement whereas, the wet medium exhibited nearly 37 percent of the original displacement obtained at 5.0 centimeters. Because USAERDL experimental data only extend to 32.0 centimeters, the curves are unreliable from the last observation to positions of greater depth. At the last observation in the dry medium negative displacements actually were obtained as plotted on Fig. 20. When these data were analyzed, serious consideration was given to the possible reflected shock that might have occurred and altered the true directions and displacements. Furthermore, in addition to the existence of the aforesaid possibility, the shock velocity of the dry medium at 30.0 centimeters was well below the sonic velocity of the medium. Hence, it would seem unlikely that a reflected shock could possess sufficient strength to alter either the direction or magnitude of the displacements.

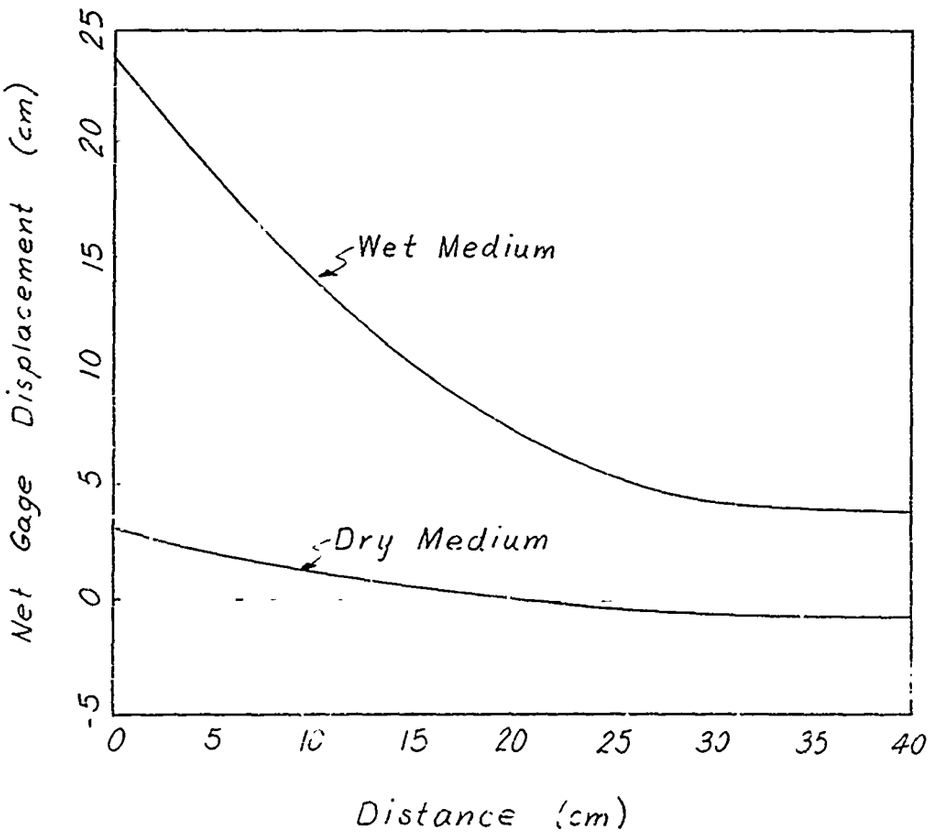

Fig. 20. Distance between bottom of charge and gage vs net gage displacement in wet and dry media.

For the dry medium, displacement data corresponding to selected depths of burst were then analyzed to determine whether depth of burst influence on net displacement was significant. With changes in depth of burst corresponding changes in net displacement were so small that no significant influence was found.

Similar analysis for the wet medium led to the conclusion that depth of burst influence on net displacement was significant. The net displacement data were then tabulated according to the depth of burst, and curves were fitted to the data as shown in Fig. 21. This figure reveals the influence the depth of burst has on net displacements at any distance from the charge. From this figure one can see that at a depth of burst of approximately 5.0 centimeters, the largest displacements occur at any distance from the charge. The remaining three depths of burst interchange their influence with increasing distance from the charge. Should further investigations reveal a similar behavior in the dry medium, then this type of

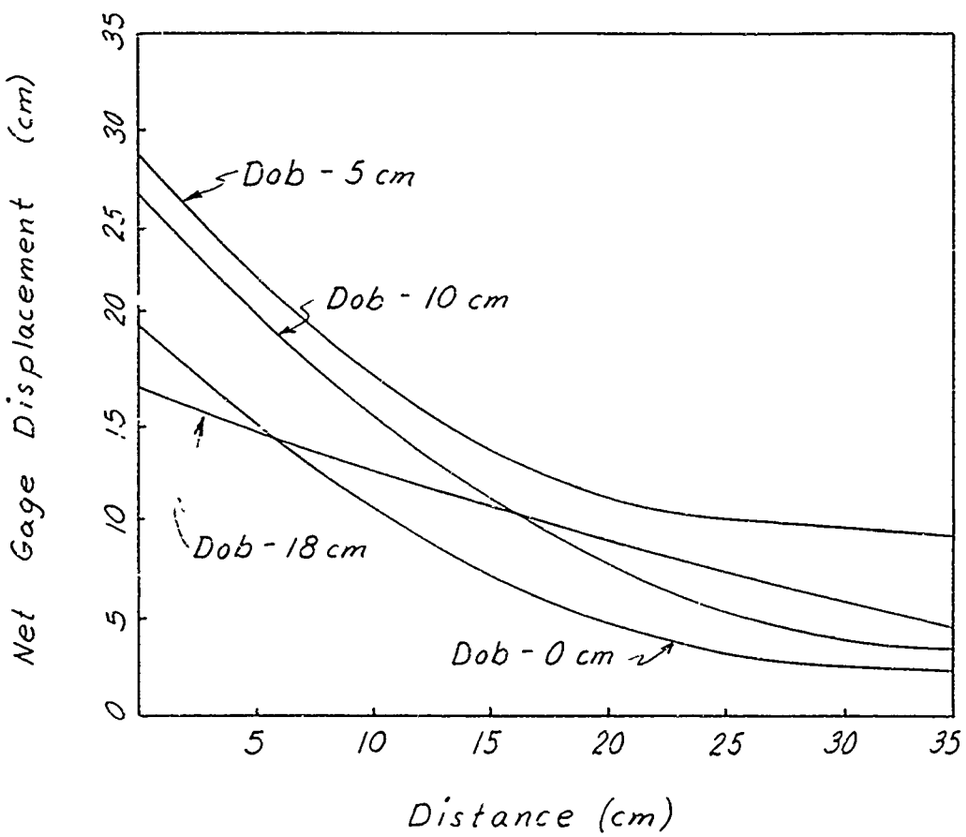

Fig. 21. Distance between bottom of charge and gage vs net gage displacement with various depths of burst in wet soil.

relationship would reveal useful displacement patterns to be expected from buried Atomic Demolitions Munitions.

In an attempt to obtain a complete understanding of the significance of the variables present, the Regression and Correlation program was used to describe the displacement behaviors in both media. The following equations

$$G_d = -0.8238(D) + 0.0182(D)^2 + 0.0839(Dob) + 8.025 \quad (18)$$

$$G_d = -1.186(D) + 0.0172(D)^2 - 0.045(Dob)^2 + 0.904(Dob) + 22.02 \quad (19)$$

and $$G_d = -0.415(D) + 1.473(M_c) - 0.0358(D)(M_c) + 0.01669(D)^2 + 0.6356(Dob) - 0.0305(Dob)^2 - 8.493 \quad (20)$$

express the displacement relationship for the dry medium, the wet medium, and the combined data of both media, respectively. The more important variables of the combined data are the distance from the charge and the moisture content, thus explaining nearly 88.0 percent of the variation in the displacement data (Appendix C, Table XIV). Insertion of the other variables brings the estimate to 95.2 percent.

Of particular interest in equation 18 for the dry medium was the inclusion of depth of burst as a significant variable. This appears to support the opinion that displacement in the dry medium would be influenced by the depth of burst just as it is in the wet medium as shown in Fig. 21.

Originally, it was expected that the variation which was obtained in the soil density might affect test results. Thus, in each of the Regression and Correlation equations the density was inserted as a variable. This variable was later eliminated because it proved to be insignificant as an explanation of the variation in the net displacements of these media.

24. Rarefaction Wave. Porzel (1) suggests that the distance from the center of the charge to the true crater depth, crushing radius, indicates the importance of the surface rarefaction wave on crater formation. A graph of the idealized behavior of this crushing radius is shown in Fig. 22.

a. At shallow depths of burst, the surface rarefaction wave overtakes the direct ground shock and reduces the ground shock pressure. Although the ground shock pressure is reduced, it still exceeds the crushing

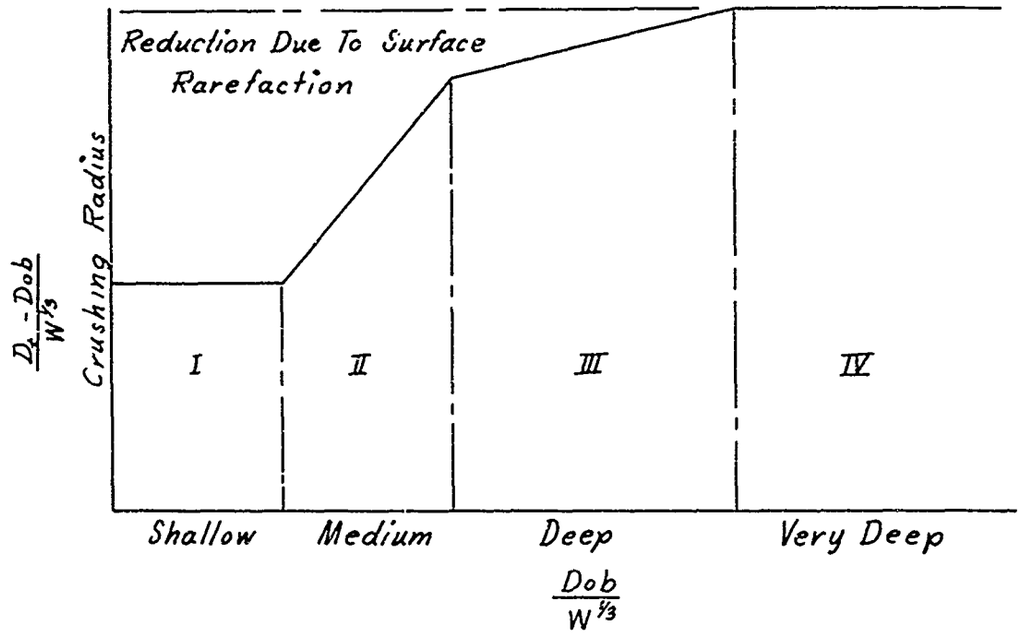

Fig. 22. Idealized scale depth of burst vs crushing radius. (Taken from Porzel's report.)

strength of the soil and produces a crushing radius less than that shown for the very deep depths of burst.

b. At medium depths, the surface rarefaction wave overtakes the ground shock at increasing distances from the charge and reduces the ground shock pressures below the crushing strength of the soil. The later arrival of the rarefaction wave results in increasing crushing radii and can be idealized by the straight line as shown for the medium depths in this figure.

c. At deep depths of burst, the direct ground shock pressure falls below the crushing strength of the soil before the rarefaction wave can overtake the ground shock. The crushing radii are reduced below that obtained for the very deep contained explosions by the amount that the ground shock is weakened by the venting of the gases from the cavity.

d. At very deep depths of burst, the maximum crushing radius is obtained, because venting of the cavity does not occur, and the ground shock is so weak upon arrival at the surface that either an extremely weak rarefaction wave or none at all is produced.

A similar plot of the dry medium data seems to behave as Porzel has suggested except for the larger camouflet radius (Fig. 23). The true crushing radius of the wet medium appears to increase rapidly to a maximum value and then gradually drops to the original value, which is approximately equal to that obtained in the camouflet. Although portions of the crushing radii in both media behave somewhat as Porzel has suggested, the data obtained by USAERDL test personnel are not sufficient or conclusive, and it would be pure speculation as to whether the behavior is the result of a surface rarefaction wave.

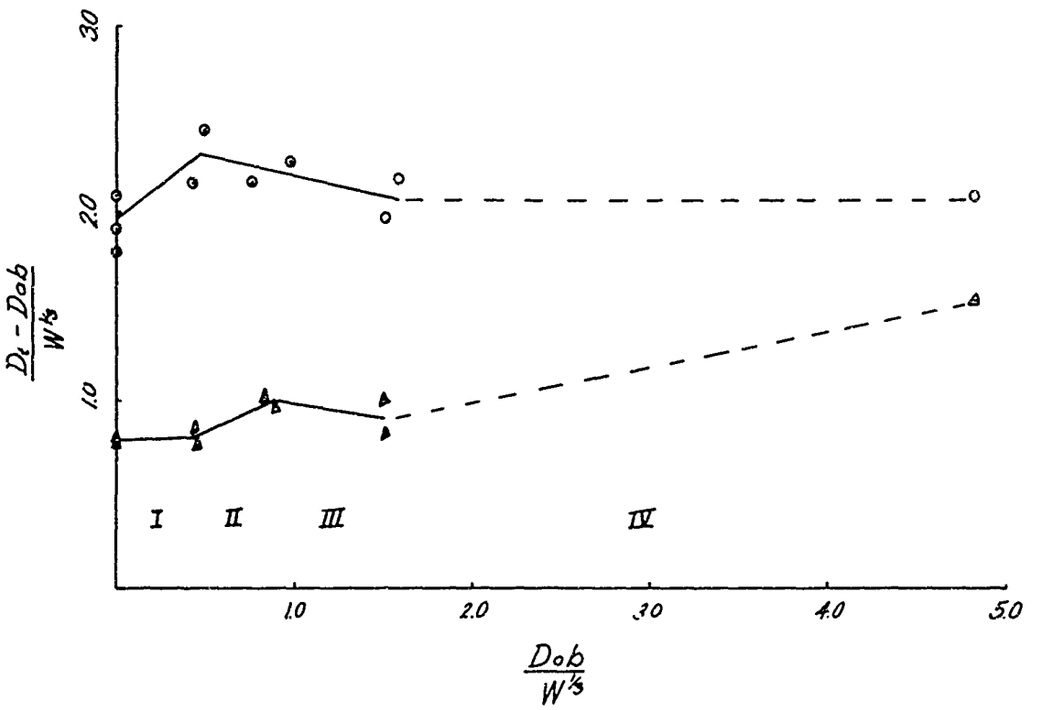

Fig. 23. Scaled depth of burst vs scaled crushing radius.

25. Soil Properties. Variations of all the soil properties occurred during the tests, and the statistical information is given in Appendix C. The engineering properties of the material have not been evaluated; hence, no relationship could be established between the engineering properties and crater behavior other than the effect moisture content has on cratering.

Based on the U. S. Army Unified Soil Classification the soil medium used in this investigation can be classified as a silty sand which exhibits a plastic index of 4.

Information should be obtained on the material properties of this soil with various moisture contents.

IV. CONCLUSIONS

26. Conclusions. It is concluded that:

a. In a cohesive soil the moist condition (moisture content within the plastic index) as contrasted with the dry condition (moisture content well below the plastic limit) influences crater formation in the following ways.

(1) Fallback into the crater is reduced so that apparent and true crater dimensions are identical.

(2) The profile of the crater is more symmetrical and parabolic in shape.

(3) The ejecta which consist of large clods, for the most part, are distributed near the crater lip.

(4) The crater parameters of depth, diameter, and especially volume are considerably increased.

(5) Attenuation rate of the shock velocity is lessened appreciably and results in higher shock velocities and pressures at greater distances from the center of the charge.

(6) Larger soil displacements are obtained at any given distance from the center of the charge.

(7) The possibility exists that a substantial increase in residual radiation may result from the lack of fallback material.

b. Large-scale results in marine muck and silty sand compared with results of this study reveal similarity in crater form. This suggests a general hypothesis that any soil which has moisture content that approaches the plastic limit will exhibit similar behavior.

LITERATURE CITED

1. Porzel, F. B., Surface Rarefaction Model for Cratering, DC58651 Washington, D. C.: Institute for Defense Analysis, May 1960.

2. Morris, P. J., "Memoranda on Anomalies in Crater Data," Nuclear Effects Branch report, USAERDL, Fort Belvoir, Virginia, May 1963.

3. Cook, Melvin A., The Science of High Explosives, New York: Reinhold Publishing Corporation, 1958.

4. U. S. Special Engineering Division, The Panama Canal, "Crater Tests in Marine Muck" ICS Memo 286-P, Diablo Heights, Canal Zone, 8 June 1948.

5. Sachs, D. C. and Swift, L. M., Small Explosion Tests, Project Mole, DC47381, Volumes I and II, AFSWP 291, Menlo Park, California: Stanford Research Institute, December 1955.

6. Bass, R. C., Hawk, H. L., and Chabai, A. J., Hugoniot Data for Some Geologic Materials, SC-4903 (RR), Albuquerque, New Mexico: Sandia Corporation, June 1963.

7. Dennis, James A., Antitank Cratering with Paste Explosives, USAERDL Report 1753-TR, Fort Belvoir, Virginia, September 1963.

APPENDIX A

AUTHORITY

RESEARCH AND TECHNOLOGY RESUME		2 GOVT ACCESSION	3 AGENCY ACCESSION	REPORT CONTROL SYMBOL
			DA Ø83718	CSCRD-103

4 DATE OF RESUME	5 KIND OF RESUME	6 SECURITY	7 REGRADING	8 RELEASE LIMITATION	9 LEVEL OF RESUME
30 04 65	A. NEW	U U	NA	GA/DC	A. WORK UNIT

10a CURRENT NUMBER/CODE	10b PRIOR NUMBER/CODE
62126011 1N022601A089 06 005 EF	NONE

11 TITLE (U) Significance of Soil Moisture and Density Changes on Ground Shock Behavior

12 SCIENTIFIC OR TECH AREA	13 START DATE	14 CMPT COMPL DATE	15 FUNDING AGENCY
011500 Nuclear Weapons Effects; 017000 Wave Propagation 015500 Soil Mechanics;	04 64	09 66	OTHER DA

16 PRODUCT METHOD	17 CONTRACT/GRANT a. NUMBER b. TYPE c. AMOUNT d. DATE	18 RESOURCES EST	a. PROFESSIONAL MAN-YEARS	b. FUNDS (In thousands)
C. IN-HOUSE	NA	PRIOR FY 64	1	$10
		CURRENT FY 65	3	$20

19 CONT LAB INSTALLATION/ACTIVITY	20 PERFORMING ORGANIZATION
NAME U. S. Army Engineer	NAME U. S. Army Engineer
ADDRESS Research and Development Laboratories Fort Belvoir, Virginia 22060	ADDRESS Research and Development Laboratories Fort Belvoir, Virginia 22060
RESP. NAME Gornak, G. TEL 703 781-8500 ext. 62206	INVESTIGATORS PRINCIPAL Gornak, G. ASSOCIATE Eaton, R., Morris, P. J. TEL 703 781-8500 ext. 62206 TYPE DA

21 TECHNOLOGY AREA(S)	22 COORDINATION
Construction; Civil Engineering	NA

23 KEYWORDS

Explosive; Cratering; Soil Moisture; Ground Shock; Soil Response

24. (U) Technical Objective - Determine the effect of moisture in soil on soil response to shock loading; and the influence of this response on ground shock behavior and crater parameters. Present, in as simple a form as possible, a technique for incorporating the militarily significant effects of soil moisture into Atomic Demolition Munitions effects prediction and employment techniques. Results will also be used in assisting research concerned with military engineering with nuclear explosives and protective structures design.

25. (U) Approach - Tests will be conducted to obtain data on the response of soil to dynamic and hydrodynamic shock loading with variations in solid, water & air fractions. Standard tests to determine engineering properties will also be conducted. A small scale HE test series will be conducted to obtain data on ground shock time-of-arrival & geometry, residual displacement, & crater parameters for varied soil conditions, & depths-of-burst. The state-of-the-art will be surveyed to make maximum use of previously conducted studies and investigations.

Present plans are to use testing methods employed previously at ERDL and by other investigators; however, these tests are sophisticated & time consuming & delays are expected. Fortunately, the conduct of one test is relatively independent of the results of any other test.

26. (U) Progress - (3 May 64 - 30 April 65) - Preliminary experiments to check experimental approaches for the cratering tests and to define to a greater degree the significance of soil moisture, were conducted in the summer & fall of 1964. Data analysis is underway and preliminary results indicate ground shock velocities, residual displacements, & crater radius & depth are greater in soil with 21% moisture content as compared to 11% moisture content. These preliminary results demonstrated the significance of soil moisture.

27 COMMUNICATIONS SECURITY	28	29 OSD CODE	30 BUDGET CODE
COMSEC OR COMSEC RELATED [X] NOT RELATED		AR	1

31 MISSION OBJECTIVE	32 PARTICIPATION
CDOG 610b(3), 1122n, USACDCNG 61-1	NA

33 REQUESTING AGENCY	34 SPECIAL EQUIPMENT

35 EST FUNDS (In thousands)	36
CY 65	

DD FORM 1 AUG 64 1498 (Items 1 to 26 identical to NASA Form 1122) REPLACES DD FORMS 613 & 613C WHICH ARE OBSOLETE

APPENDIX B

PROFILES OF RESULTING CRATERS

Depth of Burst 0.0 cm

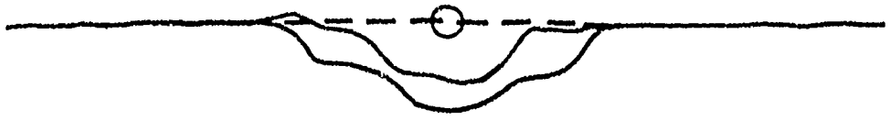

Exhibit 1

Depth of Burst 0.0 cm

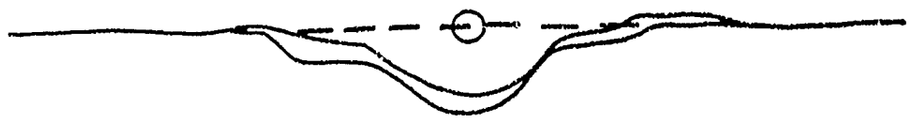

Exhibit 2

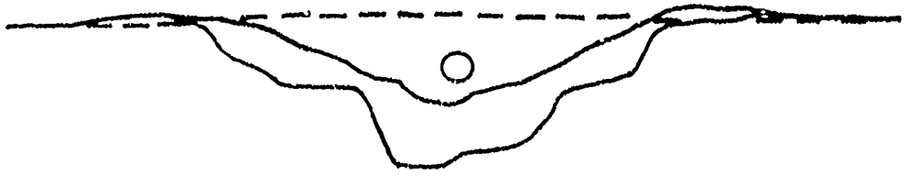

Depth of Burst 5.5 cm

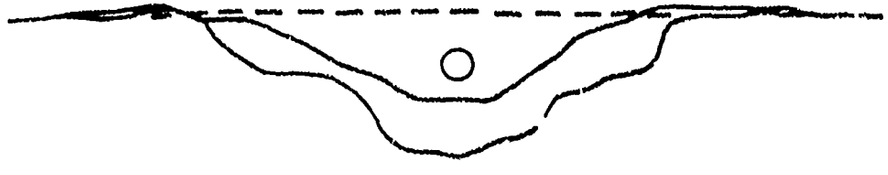

Exhibit 3

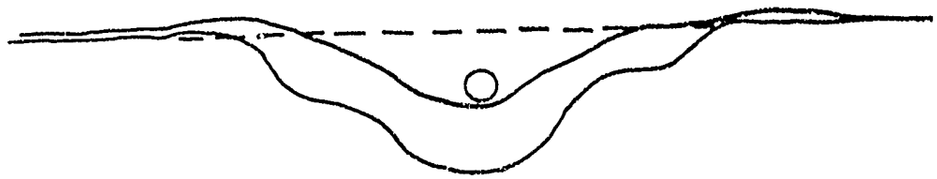

Depth of Burst 5.5 cm

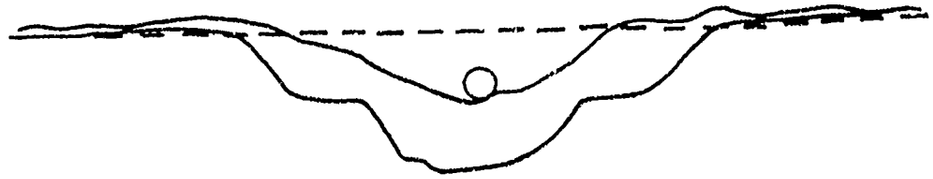

Exhibit 4

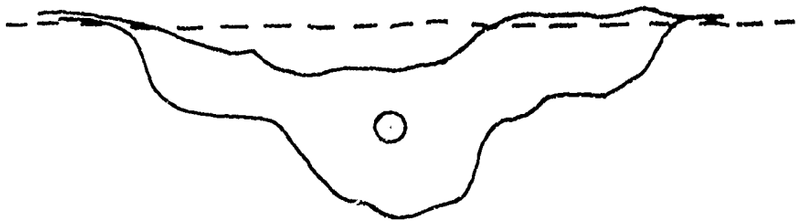

Depth of Burst 10.4 cm

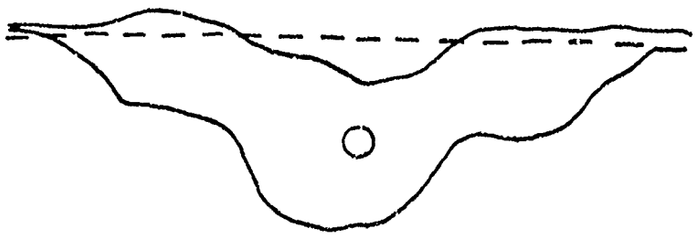

Exhibit 5

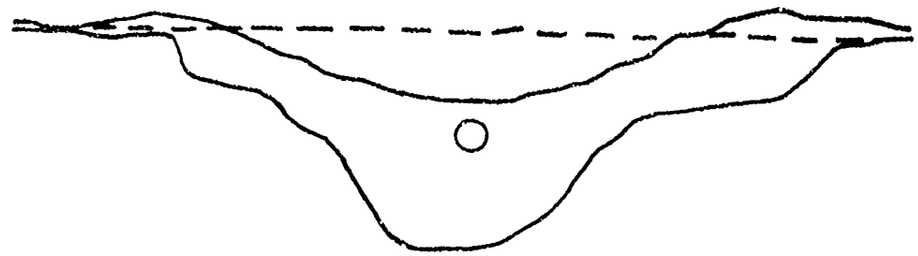

Depth of Burst 10.9 cm

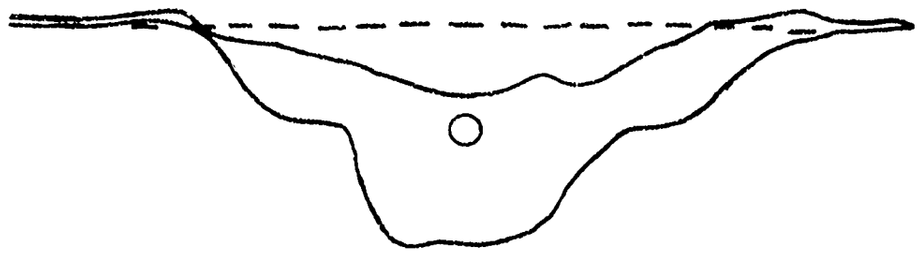

Exhibit 6

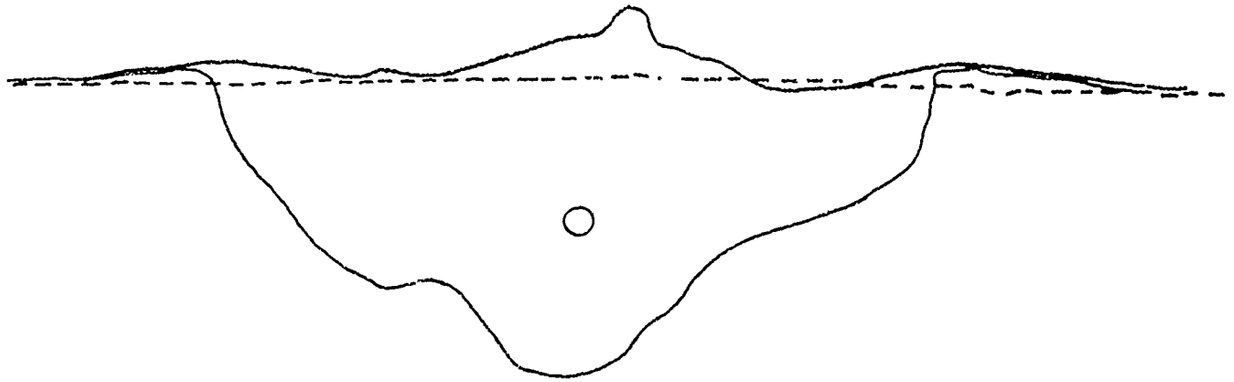

Depth of Burst 18.6 cm

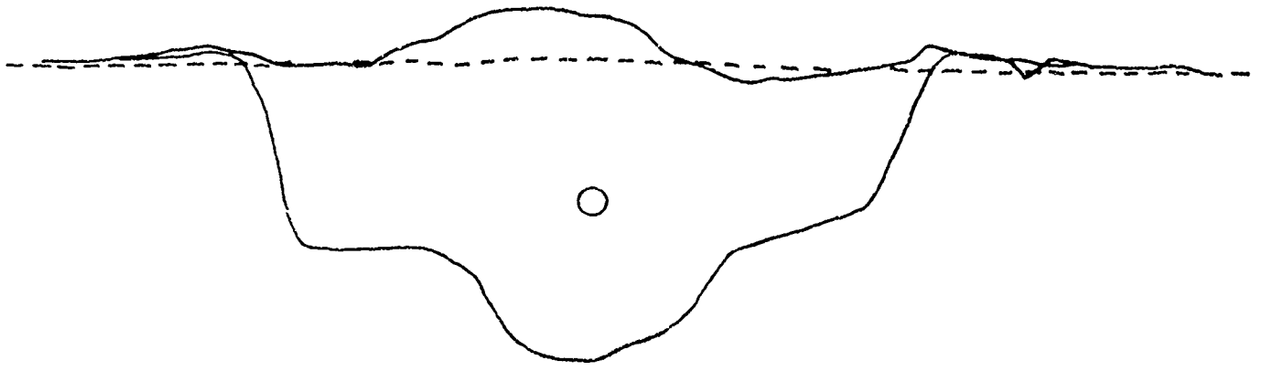

Exhibit 7

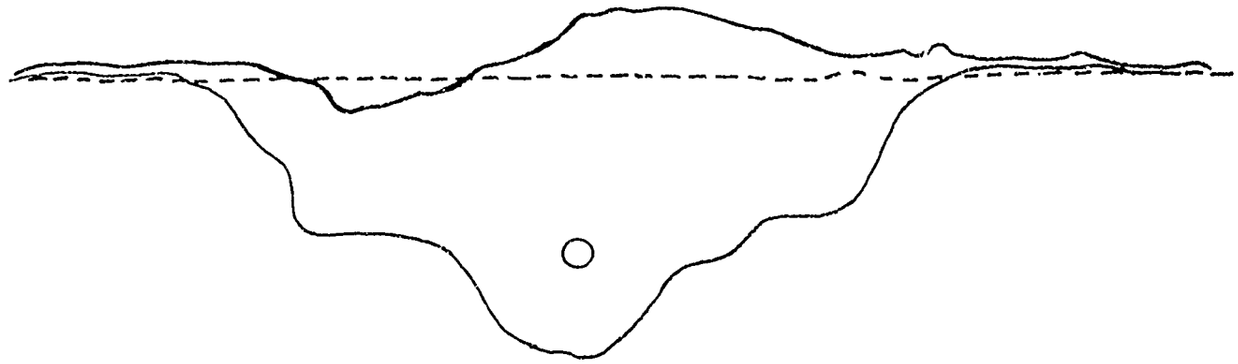

Depth of Burst 18.8 cm

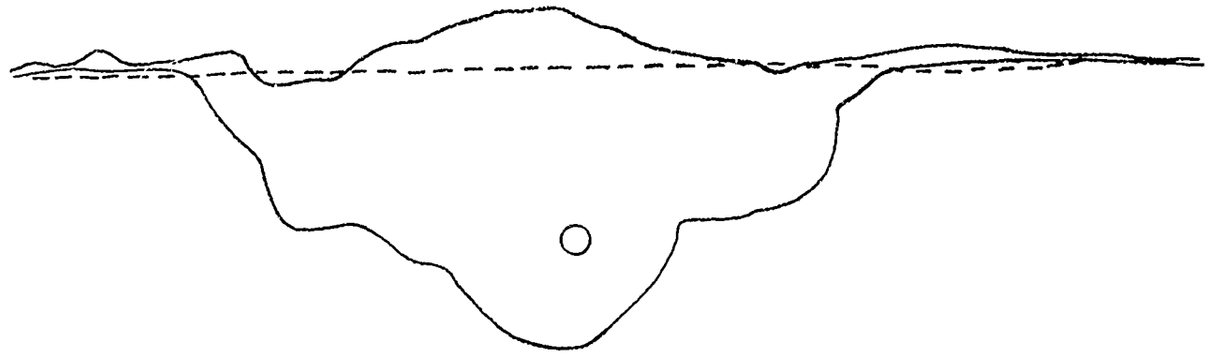

Exhibit 8

Exhibit 8

Depth of Burst 0.0 cm

Exhibit 9

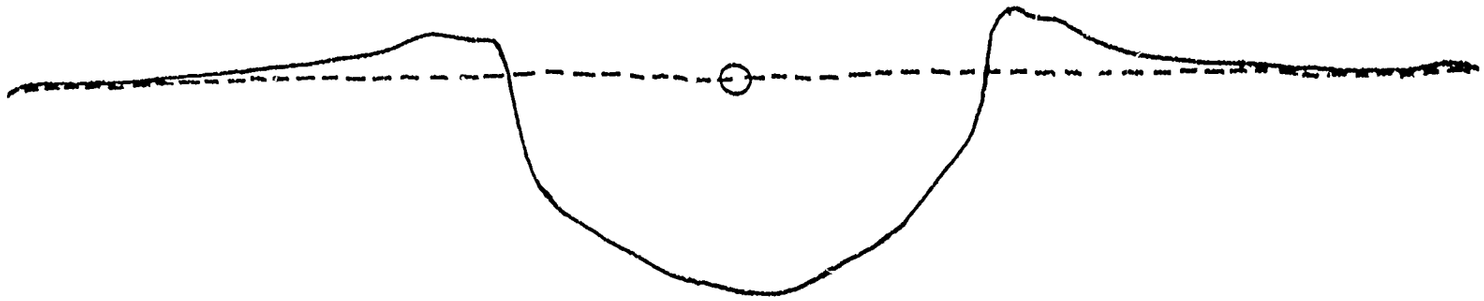

Depth of Burst 0.0 cm

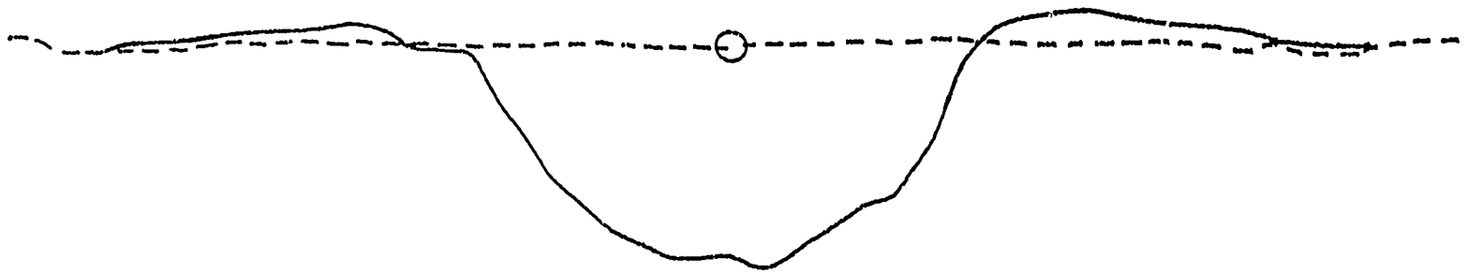

Exhibit 10

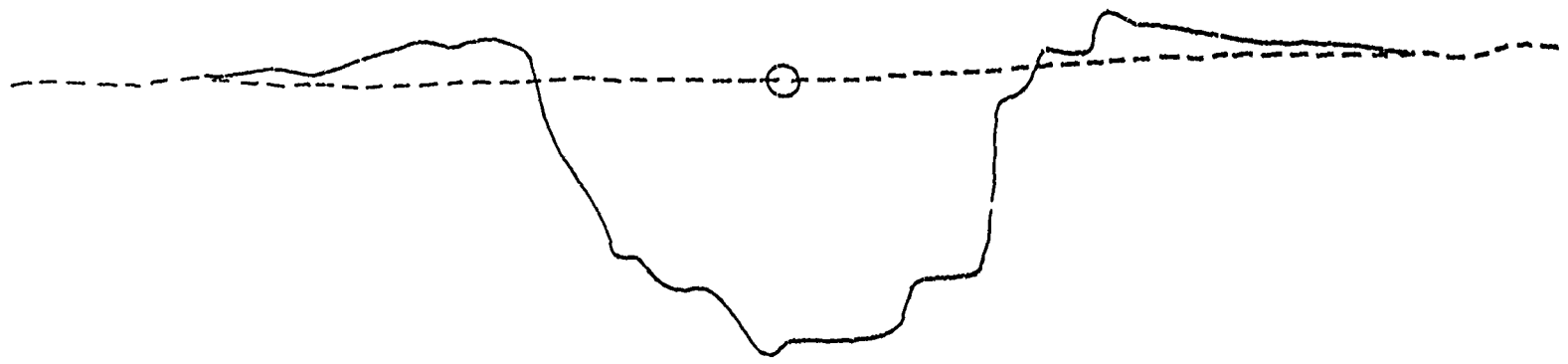

Depth of Burst 0.0 cm

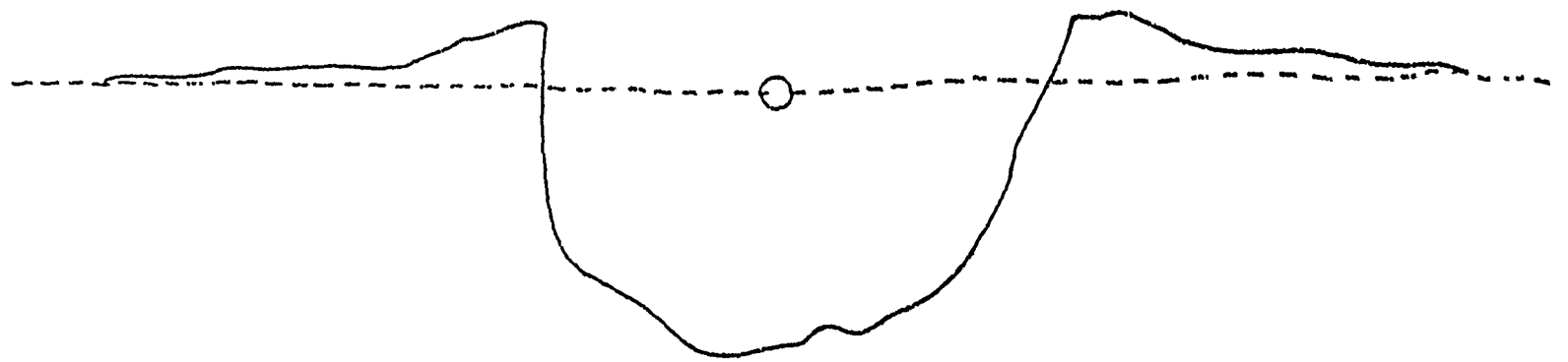

Exhibit 11

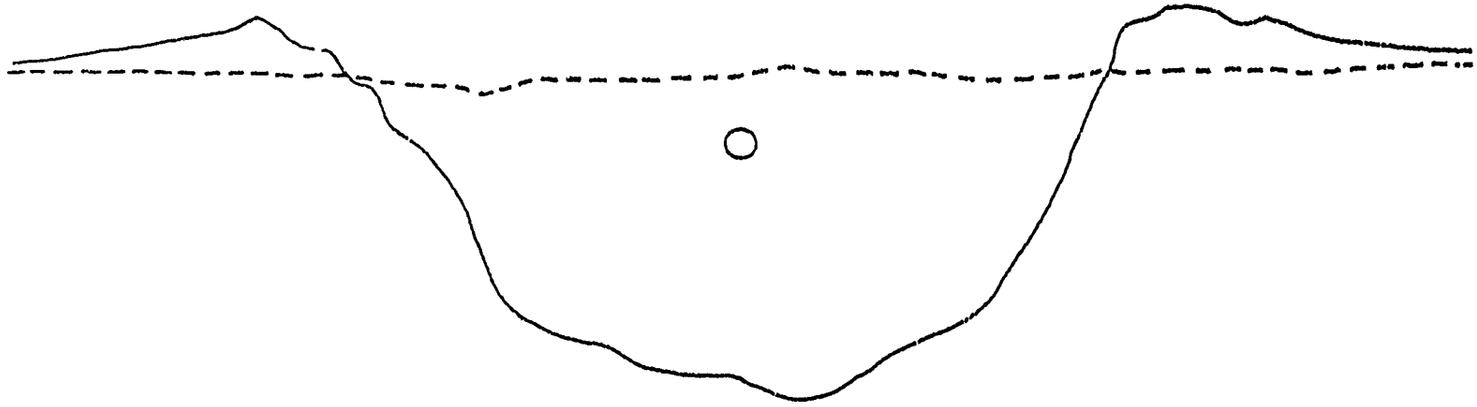

Depth of Burst 5.3 cm

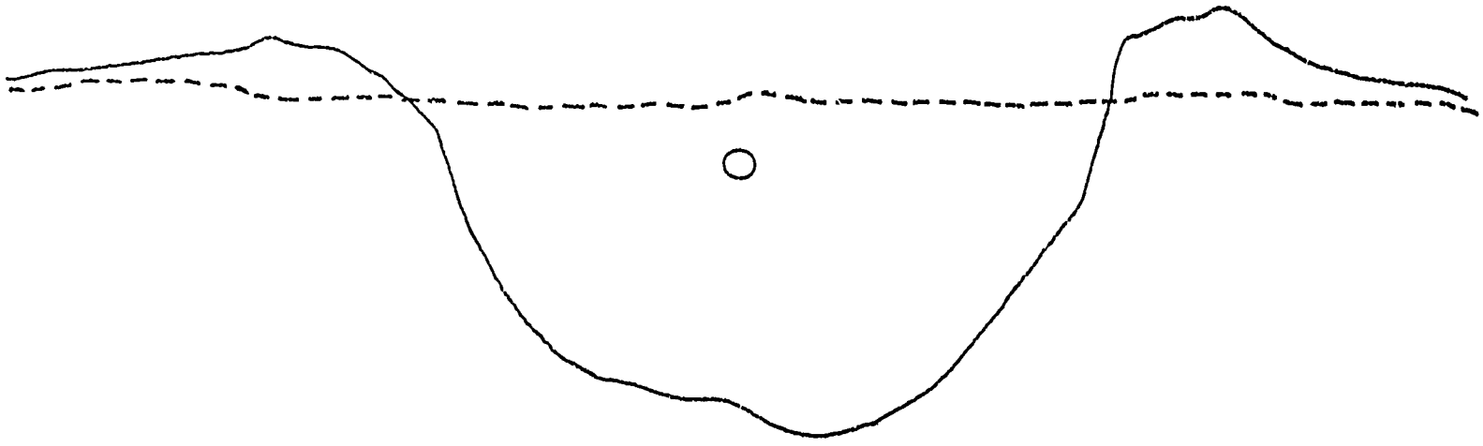

Exhibit 12

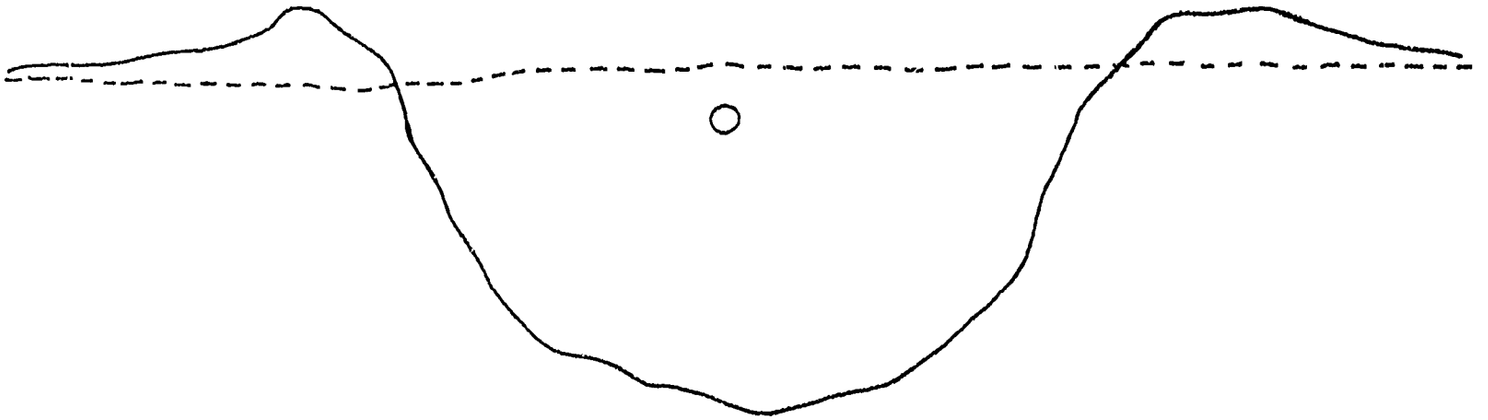

Depth of Burst 5.9 cm

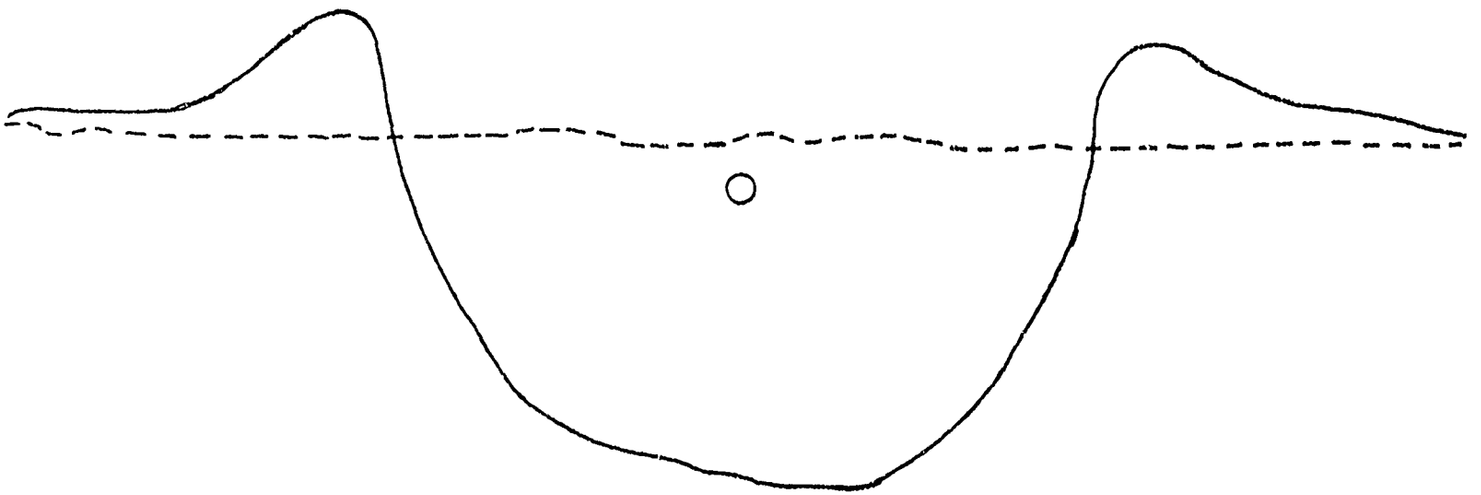

Exhibit 13

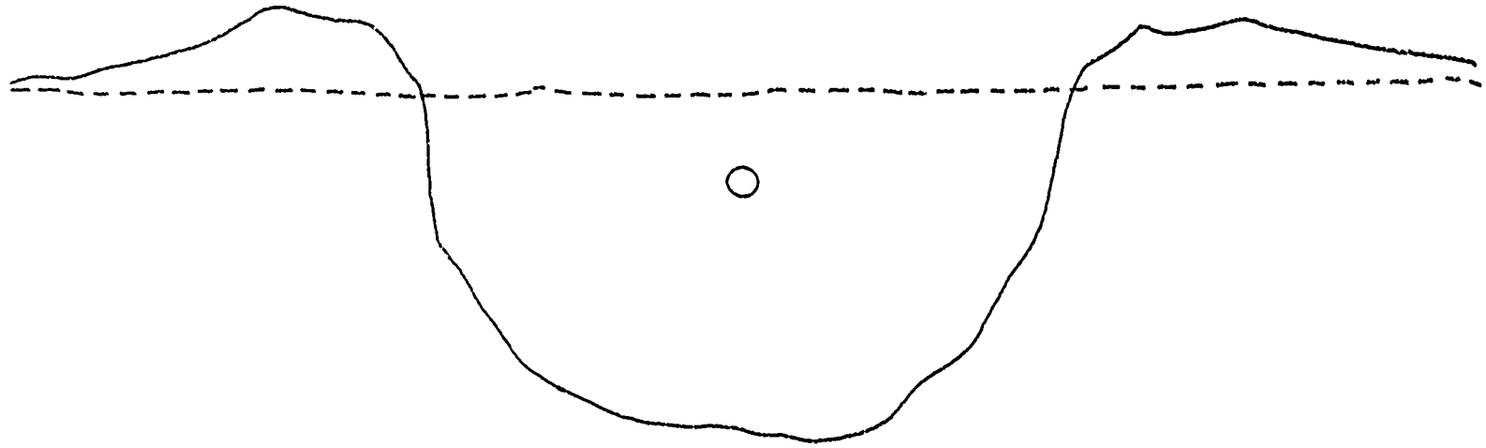

Depth of Burst 9.3 cm

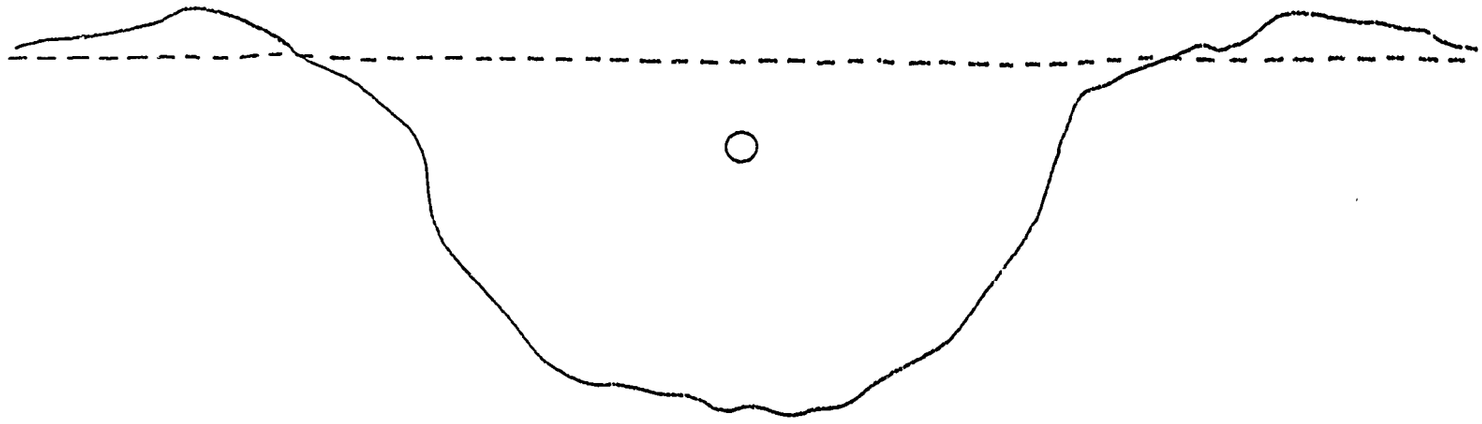

Exhibit 14

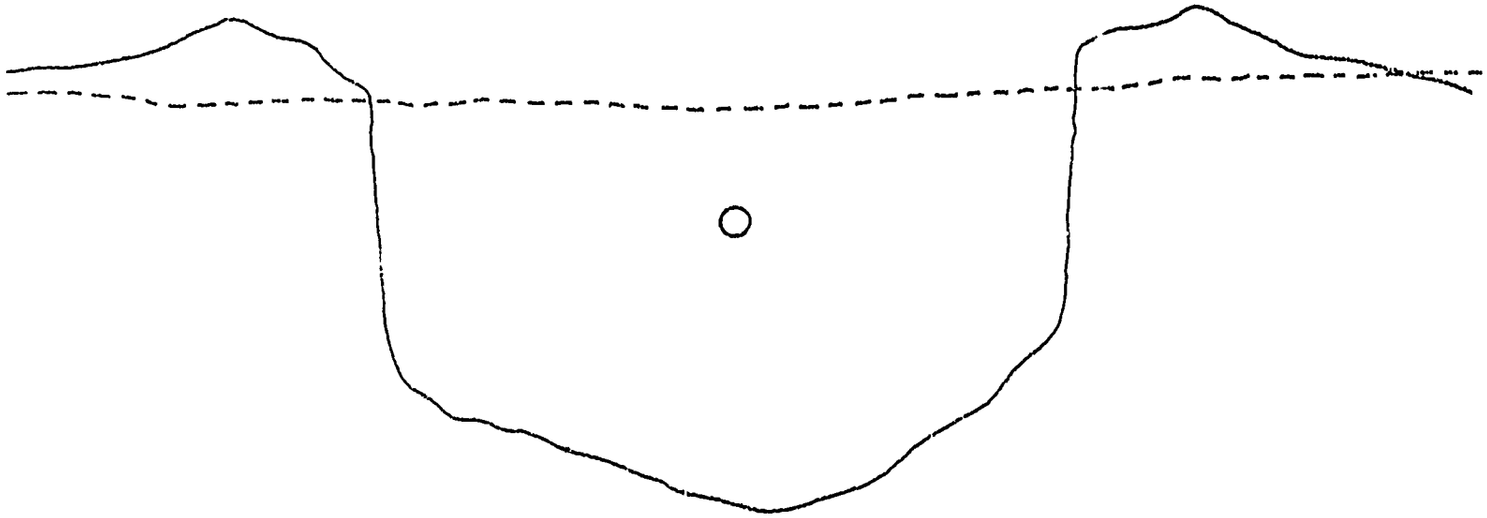

Depth of Burst 12.2 cm

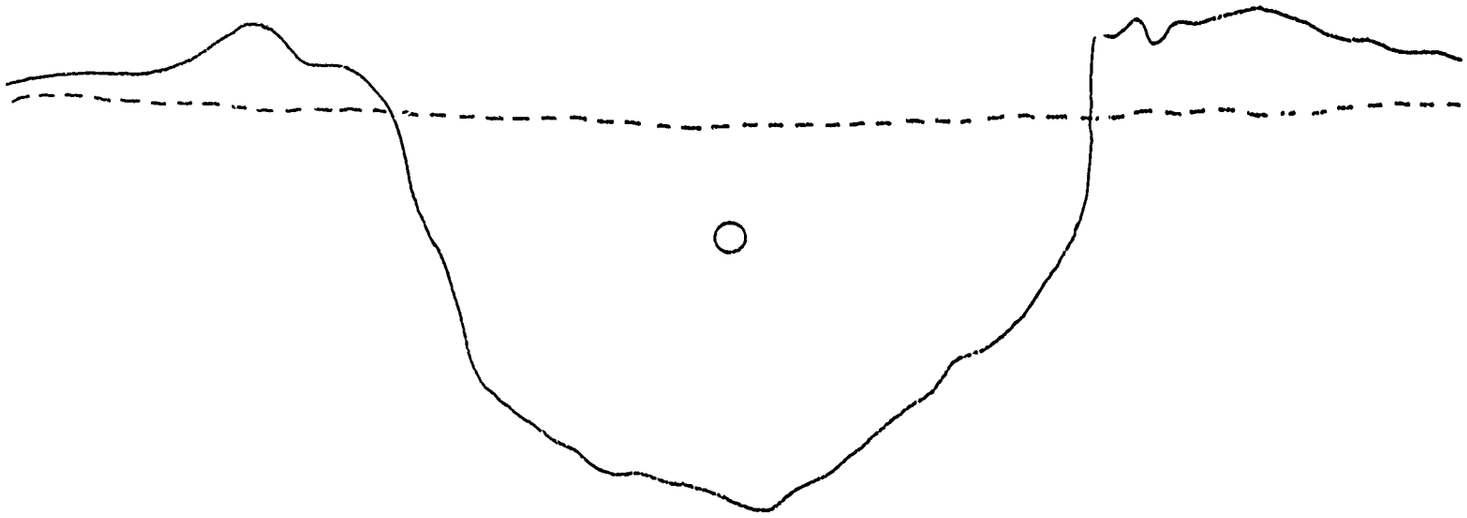

Exhibit 15

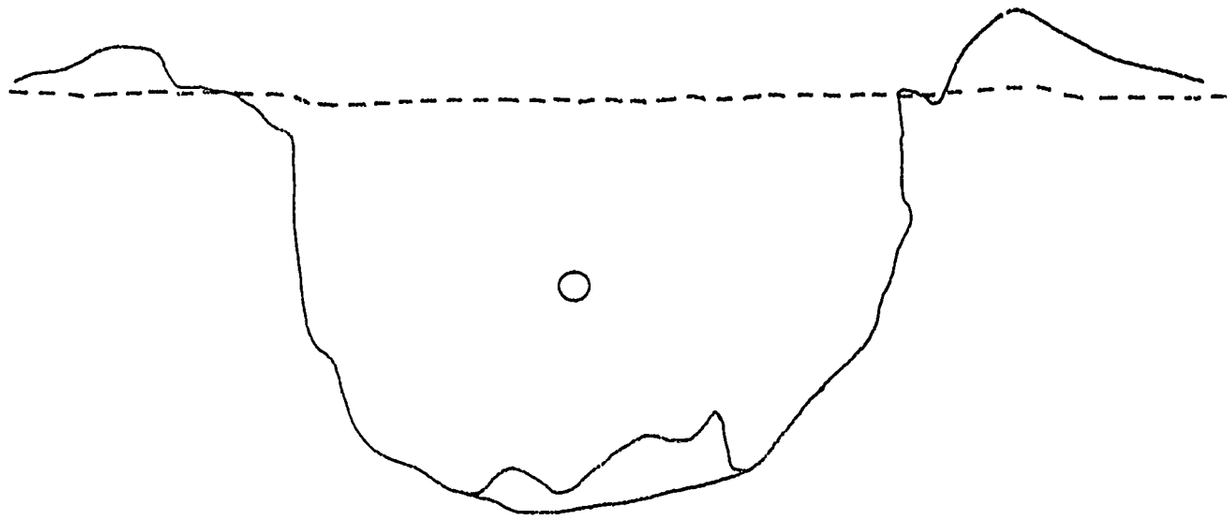

Depth of Burst 18.8 cm

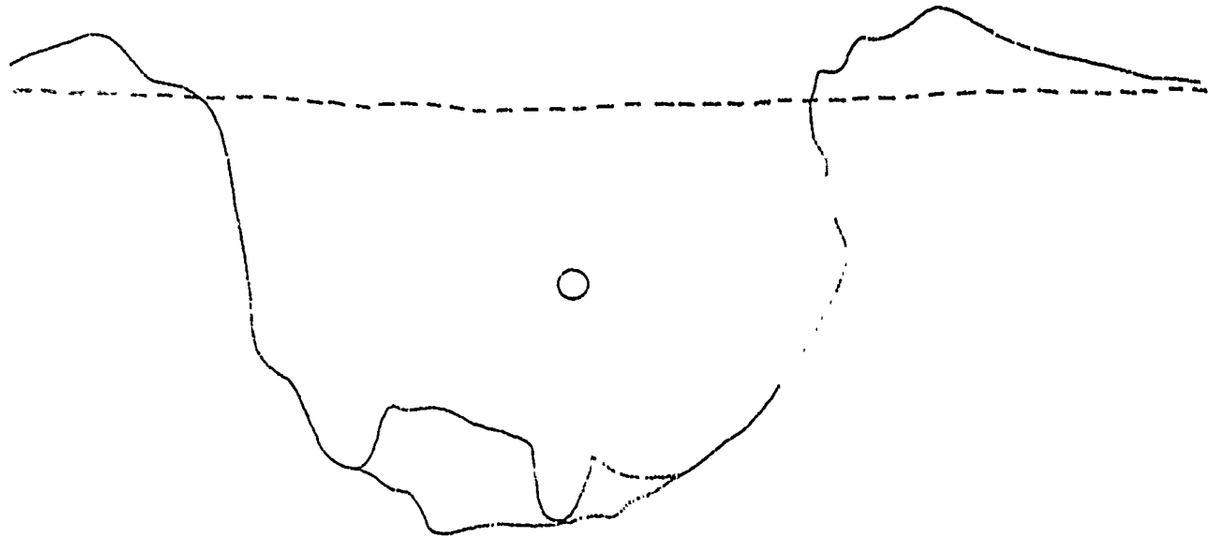

Exhibit 16

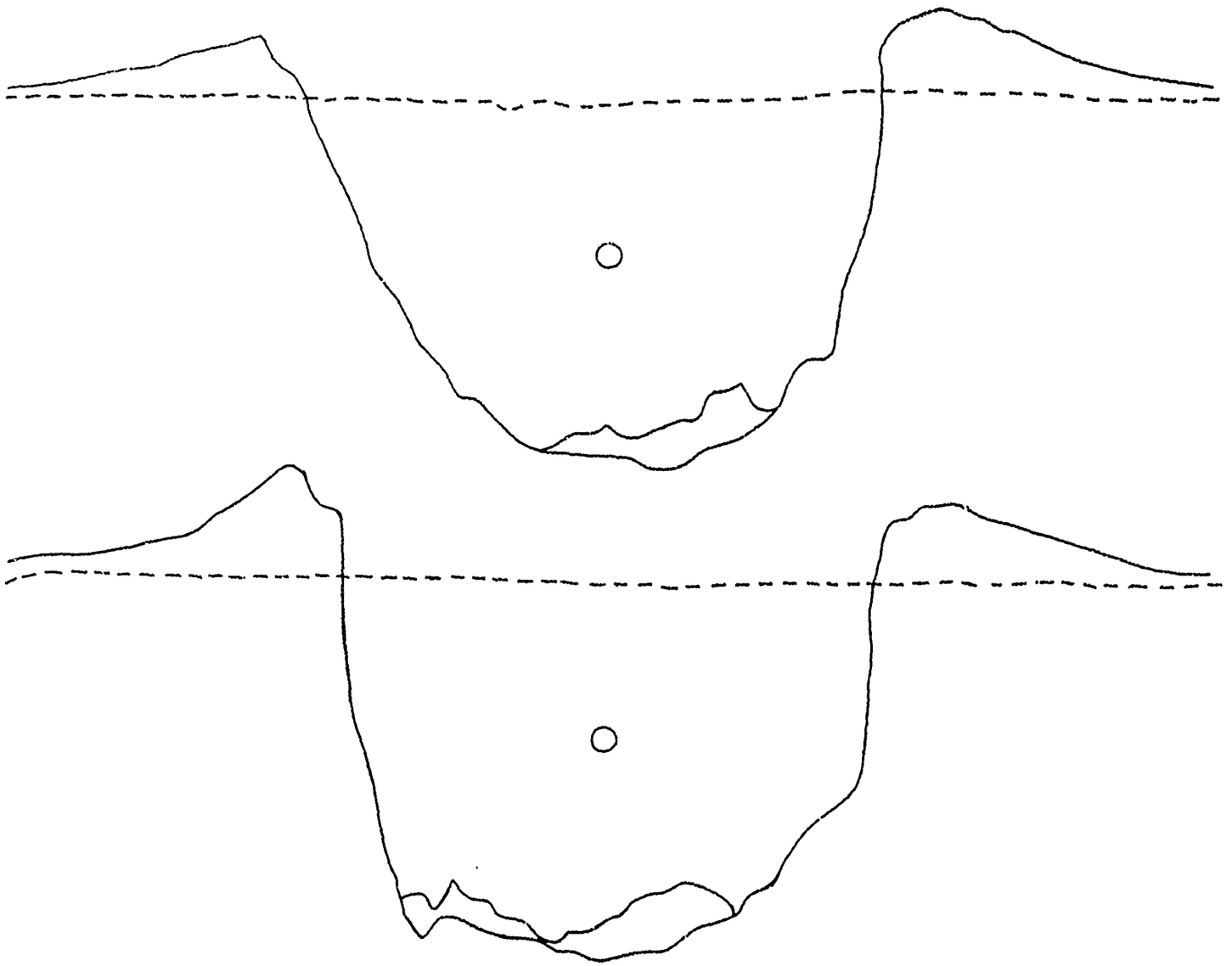

Exhibit 17

APPENDIX C

SUPPLEMENTARY INFORMATION

SUMMARY

The following report is presented to provide information on the statistical analysis of cratering data. The report concludes that:

a. Variability among the wet soil moisture content samples is significantly different, and variability among dry soil moisture content samples is homogeneous.

b. Differences among the dry soil moisture content sample means are highly significant.

c. The computed variable and confidence estimates for the cratering tests are contained in Table XIV.

d. Results indicate that no correlation exists between soil density and net gage displacement.

Table XIV. Dependent and Independent Variables with Supplementary Information on Soil Samples

Dependent Variable (Y)	Order of Occurrence Independent Variable (X)	Coefficient	Variation Explained (%)	Standard Deviation (sd)
Volume	Dob	8,163	45.7	1,389
s = 11720	% Moisture	4,318	83.5	550
R = 0.956	Dob^2	-245	91.4	70
R^2 = 0.914	C	-55,213		
Depth	Dob	1.3026	85.6	0.0827
s = 1.9200	% Moisture	1.5813	98.8	0.0049
R = 0.996	Dob(% Moisture)	-0.0140	99.3	0.1086
R^2 = 0.993	C	-7.4387		

Table XIV (cont'd)

Dependent Variable (Y)	Order of Occurrence Independent Variable (X)	Coefficient	Variation Explained (%)	Standard Deviation (sd)
Diameter	Dob	5.2501	51.7	0.7511
s = 4.6310	Dob^2	-0.1248	66.9	0.0278
R = 0.945	% Moisture	1.6693	79.8	0.3366
R^2 = 0.893	Dob(% Moisture)	-0.1006	89.3	0.0307
	C	17.1926		
Time of Arrival	D	0.0496	69.7	0.0058
s = 0.0607	D(% Moisture)	-0.0021	94.3	0.0002
R = 0.978	% Moisture	0.0107	95.2	0.0035
R^2 = 0.957	D^2	0.0003	95.7	0.0001
	C	-0.2552		
Net Gage	D	-0.4153	43.2	0.0995
Displacement	% Moisture	1.473	83.3	0.0716
s = 1.889	D(% Moisture)	-0.0358	87.9	0.0044
R = 0.976	D^2	0.0167	92.7	0.0024
R^2 = 0.952	Dob	0.6356	92.9	0.1149
	Dob^2	-0.0305	95.2	0.0057
	C	-8.4934		
Net Gage	D	-1.1855	81.9	0.1015
Displacement	D^2	0.0172	87.3	0.0032
(21.0% only)	Dob^2	-0.0450	87.5	0.0076
s = 2.0135	Dob	0.9037	93.6	0.1541
R = 0.968	C	22.02		
R^2 = 0.936				
Net Gage	D	-0.8238	71.0	0.0584
Displacement	D^2	0.0182	92.1	0.0020
(10.6% only)	Dob	0.0839	94.5	0.0281
s = 1.0040	C	8.0025		
R = 0.972				
R^2 = 0.945				

STATISTICAL ANALYSIS OF CRATERING AND SOIL DATA, DIVISION REPORT BY JAMES B. DUFF

I. INTRODUCTION

1. Subject. The purpose of this study is to analyze data from seventeen cratering experiments (test shots) to: (a) Characterize the effects of soil moisture content; and (b) determine the functional relationship between preselected cratering variables.

2. Background. The data under consideration were collected from the results of seventeen cratering tests from July to November 1964. The tests were conducted on Range 2 at USAERDL's North Annex, Fort Belvoir. Soil was selected from a site on Range 1.

II. STATISTICAL METHODS, RESULTS, AND LIMITATIONS

3. Analysis of Soil Moisture Content. Soil samples were selected at random from each of the seventeen tests. The first eight tests had, on the average, 10.6 percent soil moisture (dry), and the remaining nine had, on the average, 21.0 percent soil moisture (wet). The sample size, mean, and standard deviation for each test are listed in Table XV.

Statistical tests (0.05 level) indicate that the variability of moisture among the seventeen tests is not homogeneous. However, testing the dry and wet soils separately shows the dry soil variability is homogeneous, and that of the wet soil is heterogeneous. It can be seen from this table that tests 14 and 16 have a large amount of variability in relation to the remaining tests which could account for the lack of homogeneity.

An analysis of variance was performed on the dry soil to test for differences among shot means. The results are presented in Table XVI.

Table XV. Soil Sample Size, Mean, and Standard Deviation

Test Shot	Sample Size (n)	Sample Mean ($\bar{x}$)	Sample Standard Deviation (s)
		Soil Moisture Content (Dry)	
1	5	10.88	0.68
2	12	11.09	0.76
3	7	10.39	0.66
4	10	10.43	0.60
5	5	9.78	0.64
6	7	11.01	0.18
7	10	10.37	0.60
8	10	11.11	0.57
		Soil Moisture Content (Wet)	
9	10	20.61	0.88
10	4	21.55	0.45
11	14	21.29	0.62
12	6	20.90	0.80
13*	1	23.50	0.00
14	8	20.18	1.53
15	5	22.26	0.23
16	8	21.67	1.95
17	11	20.39	0.29

* Test shot 13 was omitted from calculations.

Table XVI. Analysis of Variance

Source of Variation	Degrees of Freedom	Sum of Squares	Mean Square	F	F 0.017,58	Expected Mean Square
Among test shots	7	11.13	1.59	4.19**	2.94	$\hat{\sigma}^2_W + 8.15\,\hat{\sigma}^2_A$
Within test shots	58	22.02	0.38			$\hat{\sigma}^2_W$
Total	65	33.15				

** Significant at 0.01 level.

From the information just presented it can be seen that the differences among shot means (moisture) are highly significant. When the expected mean squares given in this table are used, the pooled (average) standard deviation for the dry soil is computed to be 0.73 percent. [1]

Soil samples selected at random from each test were submitted to soil analysis tests. The resulting means and standard deviations are presented in Table XVII.

Table XVII. Resultant Means and Standard Deviations of Soil Samples

Parameter	No. of Test Shots (n)	Sample Mean ($\bar{x}$)	Sample Standard Deviation (s)
	Dry Soil		
Plastic Limit (%)	7	17.14	1.07
Liquid Limit (%)	7	21.57	1.81
Percent Sand (%)	7	58.99	14.53
Percent Fines (%)	7	41.01	14.53
Density, Wet (lb/ft^3)	7	109.76	5.42
Density, Dry (lb/ft^3)	7	100.70	5.06
	Wet Soil		
Plastic Limit (%)	7	17.57	0.53
Liquid Limit (%)	7	21.43	1.51
Percent Sand (%)	8	64.46	6.65
Percent Fines (%)	8	35.54	6.65
Density, Wet (lb/ft^3)	5	124.88	9.14
Density, Dry (lb/ft^3)	5	103.96	7.47

4. Cratering Effects. To determine the functional relationship between measurements obtained from the seventeen tests, regression equations were fitted by least squares. Preliminary investigations had previously been made using crater variables (volume, depth, and diameter) as the dependent variables and depth of burst (Dob) as the independent variable. Various transformations were tried, and results indicated that a polynominal

1. The pooled standard deviation was computed from: $\hat{\sigma}_T = (\hat{\sigma}_W{}^2 + \hat{\sigma}_A{}^2)^{\frac{1}{2}}$ where $\hat{\sigma}_T$ = total variability, $\hat{\sigma}_W{}^2$ = variability within shots, and $\hat{\sigma}_A{}^2$ = variability among test shots.

gave the best fit. Similar techniques were used for the dependent variables, time of arrival, and net gage displacement. Graphical presentations and respective equations for each dependent variable are exhibited in the accompanying report in Figs. 15 through 21. This information was used to indicate possible functions of the independent variable (Dob) which might be included in the fitting of the multiple independent variable model.

The final equations in this study were developed by means of an RCA "Regression and Correlation" program (90-03-006). The output consists of estimated coefficients for all independent variables, order of relative importance of the variables, multiple and partial correlation coefficients, coefficient standard deviations, and standard error about the regression surface. This output provides excellent information for observing how well the estimated equation describes a given relationship. The equations and supplemental information are presented in Table XIV.

The dependent variable, the standard error of estimate(s), and the multiple correlation coefficient (R) are listed in column one of this table. The sample standard error is the estimate of the scatter of the population about the true or population surface. If the deviations from the surface are normally distributed, about 95 percent of the points will lie within $\pm 2s$ of the surface as measured in the Y direction, Y being the direction of the dependent variable. The calculated R squared (R^2) is an estimate of the percent of variance in the dependent variable for differences in the independent variable. For example, volume has a standard deviation of 11,720 cm^3, and R^2 is equal to 0.914. For any chosen values of the independent variables one would expect the population dependent variable to fall within $\pm$ 23,440 cm^3. Also, it is estimated that 91.4 percent of the variance in volume is accounted for by the variance in the independent variables. This leaves only 8.6 percent of the variance in volume to be accounted for by all other factors.

Column two of Table XIV lists the independent variables followed by their respective coefficients in column three (the constant term, labeled c, is also listed). Column four is the percent of variation in the dependent variable accounted for by changes in the independent variable. Finally, column five lists the estimated standard deviation associated with each coefficient. It is important to note the order of occurrence for the independent variables (reading from top to bottom). Computation of the regression equation was performed by using each variable in order of its relative importance. To illustrate, take the dependent variable diameter in Table XIV. The estimated equation (column two) is read as follows:

$$\text{Diameter} = 17.1926 + 5.2501(\text{Dob}) - 0.1248(\text{Dob}^2) + 1.6693(\%) - 0.1006(\text{Dob}\cdot\%)$$

From column four it can be seen that 51.7 percent of the variance in diameter is accounted for by Dob and 66.9 percent of the variance is explained with Dob and Dob^2 until 89.3 percent is explained using Dob, Dob^2, % moisture, and the product Dob(% moisture). The standard deviation for the coefficient associated with Dob(5.2501) is given as 0.7511 centimeter in column five. An approximate 95 percent confidence interval for a coefficient can be obtained by multiplying its standard deviation by two. If the coefficient is greater in absolute value than twice its standard deviation, one is 95 percent confident that the coefficient differs from zero. Hence, 0.7511 times two equals 1.5022. Because the coefficient of 5.2501 is greater than 1.5022 one can be 95 percent confident that the true coefficient for Dob differs from zero.[2]

It was requested that the variable soil density be included in the regression models for net gage displacement. Results indicate that in all models the coefficient is equal to zero. The implication is that the range of soil density variation tested has no appreciable effect on the variance of net gage displacement, at least not in the presence of the remaining independent variables.

5. Statistical Limitations. The mathematical models used to describe the just mentioned variables were selected on the basis that they represent the best fit for the data under consideration. However, it should be noted that the cratering measurements were limited in number. In any statistical studies of this nature, the empirical equations are dependent on the adequacy of the experimental data. The many assumptions associated with the statistical tests could not be verified to a high degree because of the limited amount of data, and were, therefore, assumed to be valid.

Estimates of the probable value of the dependent variable cannot be made with any degree of accuracy for values of the independent variable extrapolated beyond the limits of the data observed; and they can be made accurately only within the range where a considerable number of observations is available.

2. Note that all coefficients meet this criterion of significance.

III. CONCLUSIONS

6. Conclusions. It is concluded that:

a. Variability among the wet soil moisture content samples is significantly different, and variability among dry soil moisture content samples is homogeneous.

b. Differences among the means of the soil moisture content samples are highly significant.

c. The computed estimates for the five dependent variables are as follows:

(1) $\text{Volume} = -55,213 + 8,163(\text{Dob}) + 4,318(\%\ \text{Moisture}) - 245(\text{Dob}^2)$

(2) $\text{Depth} = -7.4387 + 1.3026(\text{Dob}) + 1.5813(\%\ \text{Moisture}) - 0.0140(\text{Dob})(\%\ \text{moisture})$

(3) $\text{Diameter} = 17.1926 + 5.2501(\text{Dob}) - 0.1248(\text{Dob}^2) + 1.6693(\%\ \text{Moisture}) - 0.1006(\text{Dob})(\%\ \text{Moisture})$

(4) $\text{Time of arrival} = -0.2552 + 0.0496(\text{Dob}) - 0.0021(\text{D})(\%\ \text{moisture}) + 0.0107(\%\ \text{moisture}) + 0.0003(\text{D}^2)$

(5) $\text{Net Gage displacement} = -8.493 - 0.415(\text{D}) + 1.473(\%\ \text{moisture}) - 0.0358(\text{D})(\%\ \text{moisture}) + 0.0167(\text{D}^2) + 0.6356(\text{Dob}) - 0.0305(\text{Dob}^2)$

d. Results indicate that no correlation exists between soil density and net gage displacement.

UNCLASSIFIED

Security Classification

DOCUMENT CONTROL DATA - R&D

(Security classification of title, body of abstract and indexing annotation must be entered when the overall report is classified)

1 ORIGINATING ACTIVITY (Corporate author)	2a. REPORT SECURITY CLASSIFICATION
U. S. Army Engineer Research and Development Laboratories, Fort Belvoir, Virginia	Unclassified
	2b GROUP N/A

3. REPORT TITLE

PRELIMINARY EXPERIMENTS FOR CRATER MODELING IN CONTROLLED SOIL MEDIA

4. DESCRIPTIVE NOTES (Type of report and inclusive dates)

Interim Technical Report

5. AUTHOR(S) (Last name, first name, initial)

Gornak, George

6. REPORT DATE	7a. TOTAL NO. OF PAGES	7b. NO. OF REFS
June 1966	84	

8a. CONTRACT OR GRANT NO. NONE	9a. ORIGINATOR'S REPORT NUMBER(S)
b. PROJECT NO. 1N022601A089	1862
c. Task No. 1N022601A08906	9b. OTHER REPORT NO(S) (Any other numbers that may be assigned this report)
d.	

10. AVAILABILITY/LIMITATION NOTICES

Distribution of this document is unlimited.

11. SUPPLEMENTARY NOTES	12. SPONSORING MILITARY ACTIVITY
	U. S. Army Materiel Command ATTN: AMCRD-DN Washington, D. C. 20315

13 ABSTRACT This report covers a series of 30-gram, high-explosive cratering tests performed to determine effect soil moisture content in relation to the soil's plastic limit has on craters, ground shock velocities, residual displacements, and rarefaction wave.

The report concludes:

a. In a cohesive soil the moist condition (moisture content within the plastic index) as contrasted with the dry condition (moisture content well below the plastic limit) influences crater formation in the following ways. (1) Fallback into the crater is reduced so that apparent and true crater dimensions are identical. (2) The profile of the crater is more symmetrical and parabolic in shape. (3) The ejecta which consist of large clods, for the most part, are distributed near the crater lip. (4) The crater parameters of depth, diameter, and especially volume are considerably increased. (5) Attenuation rate of the shock velocity is lessened appreciably and results in higher shock velocities and pressures at greater distances from the center of the charge. (6) Larger soil displacements are obtained at any given distance from the center of the charge. (7) The possibility exists that a substantial increase in residual radiation may result from the lack of fallback material.

b. Large-scale results in marine muck and silty sand compared with results of this study reveal similarity in crater form. This suggests a general hypothesis that any soil which has moisture content that approaches the plastic limit will exhibit similar behavior.

DD FORM 1 JAN 64 1473

UNCLASSIFIED

Security Classification